CrossMark

REVIEW ARTICLE

Review: cornification, morphogenesis and evolution of feathers

Lorenzo Alibardi[1]

Abstract Feathers are corneous microramifications of variable complexity derived from the morphogenesis of barb ridges. Histological and ultrastructural analyses on developing and regenerating feathers clarify the three-dimensional organization of cells in barb ridges. Feather cells derive from folds of the embryonic epithelium of feather germs from which barb/barbule cells and supportive cells organize in a branching structure. The following degeneration of supportive cells allows the separation of barbule cells which are made of corneous beta-proteins and of lower amounts of intermediate filament (IF)(alpha) keratins, histidine-rich proteins, and corneous proteins of the epidermal differentiation complex. The specific protein association gives rise to a corneous material with specific biomechanic properties in barbules, rami, rachis, or calamus. During the evolution of different feather types, a large expansion of the genome coding for corneous feather beta-proteins occurred and formed 3–4-nm-thick filaments through a different mechanism from that of 8–10 nm IF keratins. In the chick, over 130 genes mainly localized in chromosomes 27 and 25 encode feather corneous beta-proteins of 10–12 kDa containing 97–105 amino acids. About 35 genes localized in chromosome 25 code for scale proteins (14–16 kDa made of 122–146 amino acids), claws and beak proteins (14–17 kDa proteins of 134–164 amino acids). Feather morphogenesis is periodically re-activated to produce replacement feathers, and multiple feather types can result from the interactions of epidermal and dermal tissues. The review shows schematic models explaining the translation of the morphogenesis of barb ridges present in the follicle into the three-dimensional shape of the main types of branched or un-branched feathers such as plumulaceous, pennaceous, filoplumes, and bristles. The temporal pattern of formation of barb ridges in different feather types and the molecular control from the dermal papilla through signaling molecules are poorly known. The evolution and diversification of the process of morphogenesis of barb ridges and patterns of their formation within feathers follicle allowed the origin and diversification of numerous types of feathers, including the asymmetric planar feathers for flight.

Keywords Feathers · Corneous beta-proteins · Development · Regeneration · Follicular patterns · Evolution

✉ Lorenzo Alibardi
   lorenzo.alibardi@unibo.it

[1] Comparative Histolab and Department of BIGEA, University of Bologna, via Selmi 3, 40126 Bologna, Italy

Cornification of the epidermis in vertebrates and feathers

The skin of pisciform vertebrates of the Silurian and Devonian was covered with scales, large protective, and calcium-storage dermal plaques (Maderson 1972a). This scale condition was conserved in sarcopterygian fishes and labyrinthodont amphibians from which amniotes (stem reptiles) evolved in the Upper Carboniferous (Romer 1941). While in the derived amphibians and amniote synapsids of the Permian, the scales were lost and a glandular skin evolved in the sauropsids an integument with cornified scales evolved for hydric and mechanical protection. These scales developed from folds of

Springer

the skin derived from a close association of the epidermis with mesenchymal dermal cells in forming the outer (dorsal) scale surface (Maderson and Alibardi 2000; Alibardi 2004). More complex skin appendages evolved in amniotes, such as hairs in mammals and feathers in birds (Fig. 1 S). Recent studies have definitely shown that these morphologically distinct skin appendages are homologous and they use common molecular and anatomical modules (placodes) in their development DiPoi and Milinkowitch (2016).

In the epidermis of vertebrates, keratinocytes initially accumulate intermediate filament keratins (IF keratins) and later, other specific proteins to complete their differentiation. In land vertebrates, specialized keratins richer in hydrophobic amino acids such as glycine and valine (Fuchs et al. 1987; Steinert and Freedberg 1991; Bragulla and Homberger 2009), are utilized for the formation of a corneous layer in the epidermis or epidermal derivatives, such as scales, claws, hairs, and feathers. Since intermediate filament keratins (IF keratins) produce an alpha-x ray pattern and most of the central region forms an alpha-helix these proteins were identified as alpha-keratins (Fraser et al. 1972; Fuchs et al. 1987; Fig. 1a). Other types of epidermal proteins that produce a beta-x ray pattern and are synthesized in the scales, claws, beak, and feathers of sauropsids (reptiles and birds) were termed beta- (or f-)keratins (Baden and Maderson, 1970; Wyld and Brush, 1979, 1983; Brush 1978, 1983, 1993; Gregg and Rogers 1986; Sawyer et al. 2000; Fig. 1b). Non IF keratins belong to proteins that associate with IF keratin and reinforce the keratin meshwork giving rise to harder and hydrophobic materials for the cornification of the cytoplasm (keratin-associated proteins, KAPs) and for the formation of the resistant cell corneous envelope of mature corneocytes as corneous proteins of the cell envelope (CPs, Fraser et al. 1972; Matoltsy, 1987; Powell and Rogers 1994; Kalinin et al. 2002; Candi et al. 2005). Different types of KAPs and CPs have originated in the various classes of vertebrates although only those present in some mammals (Gillespie 1991; Powell and Rogers 1994; Rogers et al. 2006) and a few proteins in birds (Powell and Rogers 1979; Knapp et al. 1991; Barnes and Sawyer 1995) are known in their amino acid sequences (Gregg and Rogers 1986; Alibardi et al. 2007, 2009). Recent studies have indicated that non-keratin, putative KAPs and other corneous proteins are present also in fish and amphibian epidermis (Alibardi 2010a; Alibardi and Segalla 2011).

Biochemical and immunocytological studies conducted in the last 10 years have shown that beta-keratins, including feather keratins do not belong to the IF family but are specialized corneous beta-proteins (CbetaPs) that evolved in sauropsids with the role of KAPs/CPs (Alibardi et al. 2007, 2009). Furthermore, recent molecular studies have shown that beta-keratins belong to a different gene family than IF keratins, and are localized in the "Epidermal Differentiation Complex" (EDC) of sauropsid chromosomes (Vanhoutteghem et al. 2008;

Mlitz et al. 2014; Strasser et al. 2014; Holthaus et al. 2015). The EDC is also present in mammalian chromosomes, and contains genes coding for other major corneous proteins of the stratum corneum but devoid of a beta-sheet region, such as involucrin, loricrin, filaggrin, etc. (Mischke et al. 1996; Kalinin et al. 2002; Candi et al. 2005).

Vertebrates derived from a common amniote progenitor, including sauropsids and mammals, utilize different types and ratios of IF keratins, KAPs, and CPs present in their EDC to build their corneous material and cell corneous envelope. In the corneous layer of sauropsids epidermis, filaments 3–4-nm thick form the hard corneous material and likely originated after the evolution of a 32–34 amino acid region present in their constitutive beta-proteins which conserve a high amino acid homology and a secondary conformation in form of beta-pleated sheets (Strasser et al. 2014; Calvaresi et al. 2016; Figs. 1b , 2S, 3S). This region acts as the filament-organizing scaffold in the formation of the bundles of hard corneous material accumulated in scales, claws, beak, and feathers (Brush 1978, 1983; Gregg and Rogers 1986; Sawyer et al. 2000; Fraser and Parry 2008, 2011). The remaining N- and C-regions of the protein make the inter-fibrillar or matrix material of the corneous material of feathers, scales, claws, and beaks. Feathers represent the more complex skin appendages, and their shape varies during their life and among species (Lucas and Stettenheim 1972; Spearman and Hardy, 1985; Chuong et al. 2003; Bartels 2003; Maderson et al. 2009). The protein composition, development, and evolution of feathers are schematically presented in the following chapters.

Major proteins of feathers

IF keratins (Fig. 1a) seem to play a lesser role than other proteins in the formation of feather barbs and barbules, but are more abundant in the calamus and rachis (Gregg and Rogers 1986; Ng et al. 2012, 2015; Rice et al. 2013; Wu et al. 2015). In fact, most of the corneous material, particularly in barbules, is composed of small proteins different from IF keratins, traditionally identified as feather keratins (Fraser et al. 1972; Haake et al. 1984; Gregg and Rogers 1986; Sawyer et al. 2000; Fraser and Parry 2008, 2011; Greenwold and Sawyer 2011, 2012, 2014; Kowata et al. 2014). These small corneous beta-proteins (CBetaPs), which genes are localized in the EDC (Vanhoutteghem et al. 2008; Mlitz et al. 2014; Strasser et al. 2014, 2015), have been selected to form most of the mature corneous material of the complex feather. Since other studies have shown that these proteins represent the specific corneous beta-proteins of feathers (Alibardi and Toni 2008; Alibardi et al. 2009; Alibardi 2013) and that their genes are located within the EDC of both birds and reptiles (Vanhoutteghem et al. 2008; Mlitz et al. 2014; Strasser et al. 2014, 2015; Holthaus et al. 2015), in the remaining part of this review, we

Fig. 1 Molecular modeling showing the different protein structure and polymerization mechanism present in IF keratins (**a**) as compared to corneous beta-protein (**b**). **a** The 4 alpha-helix of the central rod of IF keratins joined by non-alpha linker segments (*a*), form pairs (*b*), than further associate into a tretamer (*c*), octamer (*d*) forming long proto-filaments (*e*) which association form IF in the hollowed or compact model (*f*), and later form the tonofilaments (*g*). **b** the N-, C-, and the central 4 antiparallel strands of a CbetaP is shown (*a*). Only the beta-region of one protein is shown (not the N- and C-regions) (*b*) and it interacts with another beta-region to form a dimer (*c*), and six dimers interact (*d*) to form a linear growing filament made of piled dimers (*e*). The β-filament grows linearly by the progressive addition of dimers with a 45 °C rotation at each addition (*f*). The N- and C- lateral chains of each dimer form the interfilament matrix material (*gray*, *g*)
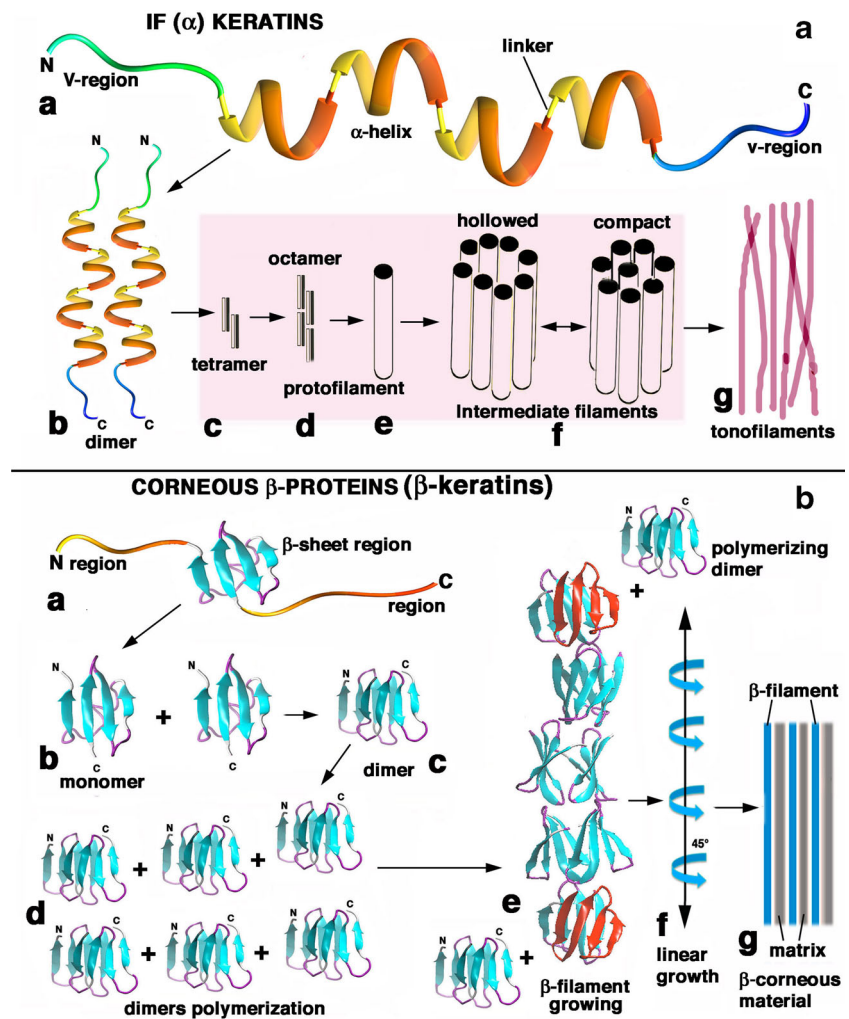
will use the term "Corneous beta-proteins" (CbetaPs) instead of the term "beta-keratins," and the term "Feather Corneous beta-proteins" (FCbetaPs) instead of the term "Feather keratins."

The central 34 amino acid-long beta-sheet region of CbetaPs includes a highly conserved 20 amino acid region, representing the core box in all sauropsid beta-proteins (Alibardi and Toni 2008; Alibardi 2013). The beta-region is considered to be the site of polymerization of beta-protein monomers to form long filaments that pack into the dense corneous material of scales, claws, and beaks (Brush 1978; Fraser and Parry 2011; Calvaresi et al. 2016; Fig. 1b). The high degree of similarity among the beta-region in sauropsid CbetaPs suggests that this beta-region was already present in the sauropsid ancestor around 320 millions years ago. In the subsequent evolution, the beta-sheet region has maintained a high similarity in various reptilian and avian groups, reflecting its essential role in the formation of the beta-keratin filaments (Calvaresi et al. 2016). While in IF keratins and in the KAPs/CPs so far known, no central beta-sheet regions are present, the beta-region of CbetaPs determines the formation

of filamentous polymers with a completely different mechanism from than that of IF keratins (Fig. 1a, b). In IF keratin filaments, the interactions between the central alpha-helix region and the lateral regions of two monomers (types I and II, see Coulombe and Omary 2002; Bragulla and Homberger 2009) give rise to a dimer, then to a tetramer and eventually, to a proto-filament that associates into eight peripheral proto-filaments (in epidermal keratins), or into seven peripheral proto-filaments surrounding one central proto-filament (in hair keratins). This organization gives rise to the IFs of 10–12 nm in diameter, which associate with other filaments forming bundles or tonofilaments (Fig. 1a).

In contrast to IF keratins, in CbetaPs, the central region of 34 amino acids initially gives rise to a homo-dimer (the N- and C-regions remain outside this nucleation region) due to specific polar and apolar bonds within the beta-regions of two monomers (Fig. 1b). Next, the dimers pile up into a linear filament of 3 nm due to hydrogen and van der Waals bonds (Calvaresi et al. 2016). Each dimer is bonded over the previous dimer with a rotational angle of about 45° along a right-handed axis so that, when four dimers are repeated along the axis, the

position of the beta-sheets is conserved (same red-colored beta-sheets shown in Fig. 1b, e; but see details in Calvaresi et al. 2016). As mentioned earlier, the N- and C-regions of the monomers and dimers remain peripheral to the elongated axial filaments, forming the inter-fibrillar- or matrix-material (Fraser and Parry, 1996, 2008). These lateral N- and C-regions are specific for each sauropsid group, lepidosaurians, turtles, and archosaurians (Alibardi et al. 2009; Fraser and Parry 2011; Greenwold and Sawyer 2014), and were likely added and/or changed in the individual lineages of derived reptiles (turtles, crocodilians, birds, lizards, and snakes) to fulfill specific roles in their epidermis.

Corneous beta-proteins of sauropsid scales, claws, and beaks

Originally the skin of lepidosaurs and archosaurs was probably scaled with different patterns (Maderson 1972b; Martin and Czerkas 2000; Maderson and Alibardi 2000; Sumida and Brochu 2000; Coria and Chiappe 2007). Both scales and claws (Maddin and Reisz 2007) probably utilized small CPs that originated in the reptilian integument possibly in the Upper Carboniferous (Strasser et al. 2014; Calvaresi et al. 2016). These proteins of 13–17 kDa, comprise 89–184 amino acids in lizards and snakes (Dalla Valle et al. 2005), 2007a, 2007b, 2009a. In turtles, they are 12–17 kDa proteins comprising 122–174 amino acids (Dalla Valle et al. 2009a, 2009b), and in crocodilians, they are 17–20 KDa proteins, comprising 179–203 amino acids (Dalla Valle et al. 2009c). Finally in birds, these proteins comprising 139–150 amino acids in claws and scales possess a molecular weight of 14–16 kDa (Gregg and Rogers 1986; Sawyer et al. 2000). In contrast to feather beta-proteins, those of scales, beaks, and claws possess a variably long glycine-rich region, the C-terminal, which allows the classification of the non-feather and feather proteins (Figs. 2S and 3S, even though the specific expression region of most of these proteins is not known yet; see Ng et al. 2014; Kowata et al. 2014; Wu et al. 2015).

The resulting CbetaPs of archosaurian scales, claws, and beaks contain a N-region rich in cysteine, followed by a core box located in an anterior region of the molecule, and by a variably long and hydrophobic glycine-rich tail (Fig. 2S). Also, valine and tyrosine are present, and they contribute to making these proteins less soluble and more hydrophobic. Toward the C-terminus of the protein, a variable number of cysteines are present, which probably form cross-links among beta-proteins or with IF keratins. The mechanical resistance and hydrophobic character of scales, claws, and beaks derives from the richness in hydrophobic amino acids such as glycine, valine, and tyrosine in addition to the cross-linking cysteines located in the N- and C-regions (Fraser and Parry 2014).

The number of CbetaPs present in scales of turtles and crocodilians varies from 20 to 90 (Dalla Valle et al. 2009a, 2009b, 2009c; Greenwold and Sawyer 2011, 2013; Li et al. 2013; Holthaus et al. 2015). Present genomic and proteomic analysis of epidermal proteins of crocodilians and turtles (Alibardi and Toni 2006; Toni et al. 2007; Alibardi 2009a, b, Alibardi 2010a) have indicated that the number of corneous beta-proteins in different reptiles is related to the number of skin appendages (e.g., different types of scales, claws, and other appendages) or to the intrinsic complexity of the epidermis (multilayered as in lepidosaurians or simpler as in crocodilians and turtles). Since feathers are the most complex skin appendages present in vertebrates, it is likely that a higher number of feather beta-proteins is present in comparison to those needed for the other, simpler appendages (scales, claws, and beak). In fact, the total number of CbetaPs genes detected in the genomes of birds is above 120 (Alibardi and Toni 2008; Greenwold and Sawyer 2010, 2011, 2011, 2013; Greenwold et al. 2014, see numerous examples in Fig. 3S).

Corneous proteins of feathers

In the chicken genome, at least 36 genes for scale, claw, and beak CbetaPs are present, and the longer proteins (130–150 amino acids) are located mainly in chromosome 25 (Alibardi and Toni 2008; Greenwold and Sawyer 2010; 2011; 2013; Greenwold et al. 2014, see numerous examples in Fig. 2S). Although expression data for most of these proteins are not known, the presence of glycine-rich regions after the core box suggests that these CbetaPs are expressed in non-feather appendages as indicated by Ng et al. (2015) and Wu et al. (2015). Conversely, feather corneous beta-proteins (FCbetaPs or feather keratins) show a reduction or complete loss of these glycine-rich regions (Gregg and Rogers 1986; Fig. 3S).

During embryogenesis in the alligator, chick, and zebra finch, the subperiderm layer (the third layer of keratinocytes produced in the embryo (Sawyer et al. 2003, 2005; Sawyer and Knapp 2003; Alibardi et al. 2006) accumulates CbetaPs, including a protein possessing an epitope characteristic for feathers. This observation shows that the embryonic archosaurian epidermis is capable of producing FCbetaPs in addition to other CbetaPs. The interpretation of this observation is that during avian evolution, the glycine-rich region might have been added to the short precursor of both feather and scale proteins to evolve scale and claw beta-proteins. Therefore, the specific genes for scale, claw, beak, and feather beta-proteins are activated in different areas of the skin of a bird during its life according to their specific morphogenetic program. Proteomic data indicate that a large heterogeneity of feather beta-proteins is present in the different parts of feathers (Brush 1978, 1986; Gregg and Rogers 1986; Ng et al. 2012, 2015; Rice et al. 2013; Greenwold et al. 2014; Wu et al. 2015).

In feathers, beta-keratins rapidly replace the few alpha-keratin filaments present at the beginning of differentiation of feather cells (Bell and Tatachari, 1963; Matulionis 1970; Meyer and Baumgartner 1998; Alibardi 2002, 2009a, 2013; Alibardi and Toni 2008) so that mature feather cells, especially in barbs and barbules, show little, if any, alpha-keratin content or x-ray alpha-pattern (Filsie and Rogers 1961; Baden and Maderson, 1970; Kemp et al. 1974). The initial, electron-dense small bundles made of few 8–10 nm-thick IF keratin filaments synthesized in barbule and barb cells (Filsie and Rogers 1961; Matulionis 1970; Alibardi 2002, 2013; Alibardi and Toni 2008) are rapidly coated by the deposition of large amount of the smaller FCbetaPs, forming large bundles or packets of amorphous and more electron-pale material, traditionally indicated as feather keratin but actually representing corneous bundles containing several proteins in addition to the prevalent FCbetaPs. When observed at high magnification, this corneous material shows an irregular filament pattern of 3–4 nm in diameter (Filsie and Rogers 1961; Kemp et al. 1974; Fraser and Parry 2008; Alibardi 2013).

In contrast to the proteins of scales, claws, and beaks, feather beta-proteins have a deletion of 52 amino acids in the C-terminal region (Gregg et al. 1983, 1984; Gregg and Rogers 1986). Feather beta-proteins are formed by only 97–105 amino acids, and this shortening initially suggested that feather proteins derived from scale proteins during evolution (Gregg et al. 1984; Gregg and Rogers 1986). Most glycines form loops that somehow interfere with the linear framework of the filament of beta-keratin, and the elimination of the glycine-rich regions and the smaller dimension make feather proteins capable to form the elongated bundles of corneous material present in barb and barbule cells. The absence of the glycine-rich sequences (compare the post-core box regions in most of the sequences in Figs. 2S and 3S) probably allows a more direct interaction of monomers that facilitate the formation of organized bundles of feather filaments with respect to the more irregular orientation of the bundles of scales, claws, and beak filaments (Gregg and Rogers 1986; Fraser and Parry, 1996; 2008; Calvaresi et al. 2016).

Although these molecular data support the derivation of feathers from scales (Maderson 1972b; Greenwold and Sawyer 2010), other embryological observations (Sawyer et al. 2003; Prin and Dhouailly 2004; Alibardi et al. 2006; Dhouailly 2009) and phylogenetic analyses (Gregg et al. 1983; Dalla Valle et al. 2008; Greenwold and Sawyer 2011, 2013, 2014) suggest the possibility that the short and specialized CbetaPs of feathers evolved from a common sauropsid ancestor independent from scale proteins. It was proposed that the common progenitor protein present in a basic reptilian ancestor could be derived from the assemblage of smaller peptides, some containing the beta-pleated region and others the external regions (Brush 1993). After this gene was duplicated, one copy might have been maintained or refined the glycine-rich tail region (scales, claw, and beak proteins) while in the other copy, the region coding for the glycine-rich region was deleted giving rise to the smaller feather proteins.

Past and the recent molecular studies have indicated that feathers are composed not only of FCbetaPs (feather keratins) but also of IF keratins and non-beta corneous proteins of the EDC (Alibardi and Toni 2008; Ng et al. 2014; Greenwold and Sawyer 2010, 2011; Greenwold et al. 2014; Strasser et al. 2015). The genes for IF keratins are relatively few, less than 40 in the chick genome, and only few of these IF keratins are found in feathers (Fig. 2). These genes contain 8–9 coding exons separated by introns (Fig. 2a, b). Conversely, many more CbetaPs are found in feathers, encoded by numerous genes most located in the EDC. Each gene is made of 2 exons separated by a single intron, with only part of the second exon encoding (Gregg and Rogers 1986; Fig. 2c, d). The initial screening of the chick genome (Dalla Valle 2007, unpublished data; Alibardi and Toni 2008) showed that most of claw, scale, beak, and feather keratin genes (at least 107 in the chick genome, completely or partially lacking the glycine-rich tail region), are located in chromosome 27 (67 genes), and in chromosome 25 (24 genes), while a few feather genes are present in chromosomes 1 (1 gene), 2 (7 genes), 5 (1 gene), 6 (3 non-feather genes), 7 (1 gene), and 10 (3 genes). Similar figures were also found in the chick and other birds (Glenn et al. 2008; Greenwold and Sawyer 2010, 2011, 2013; Greenwold et al. 2014; Ng et al. 2014; see numerous examples in Fig. 3S). The location of so many feather protein genes on chromosome 27 indicates an intense process of gene duplication and mutation that might have occurred during bird evolution. This process was probably related to the increase in feather types during ontogenesis and in adult life, such as in natal downfeathers, juvenile feathers, adult feathers of different types (e.g., plumulaceous feathers, pennaceous feathers, filoplumes, and bristles). The analysis of most beta-keratin genes in the chick genome and of the related proteome (Rice et al. 2013) shows that most (74 %) of these structural proteins are represented by feather keratins, while relatively few genes are coding for scale, claw, and beak beta-proteins (see examples of CbetaPs shown in Figs. 2S and 3S). The numerous variants probably represent specialized FCbetaPs utilized in different types of feathers formed during the development and post-natal life of the chick, but specific expression studies are still incomplete (Ng et al. 2014; Wu et al. 2015). Variations in FCbetaPs are also present in modern bird orders, suggesting that the evolution of genes coding for these proteins is still active (indicated as feather beta-keratins in Glenn et al. 2008).

The map of IF keratins and CbetaPs distribution derived from different studies (Ng et al. 2012, 2014; Greenwold et al. 2014; Wu et al. 2015; Fig. 2e) indicates that some proteins contribute to the progressive maturation and hardening of barbule and barb cells, while other proteins are likely more suited
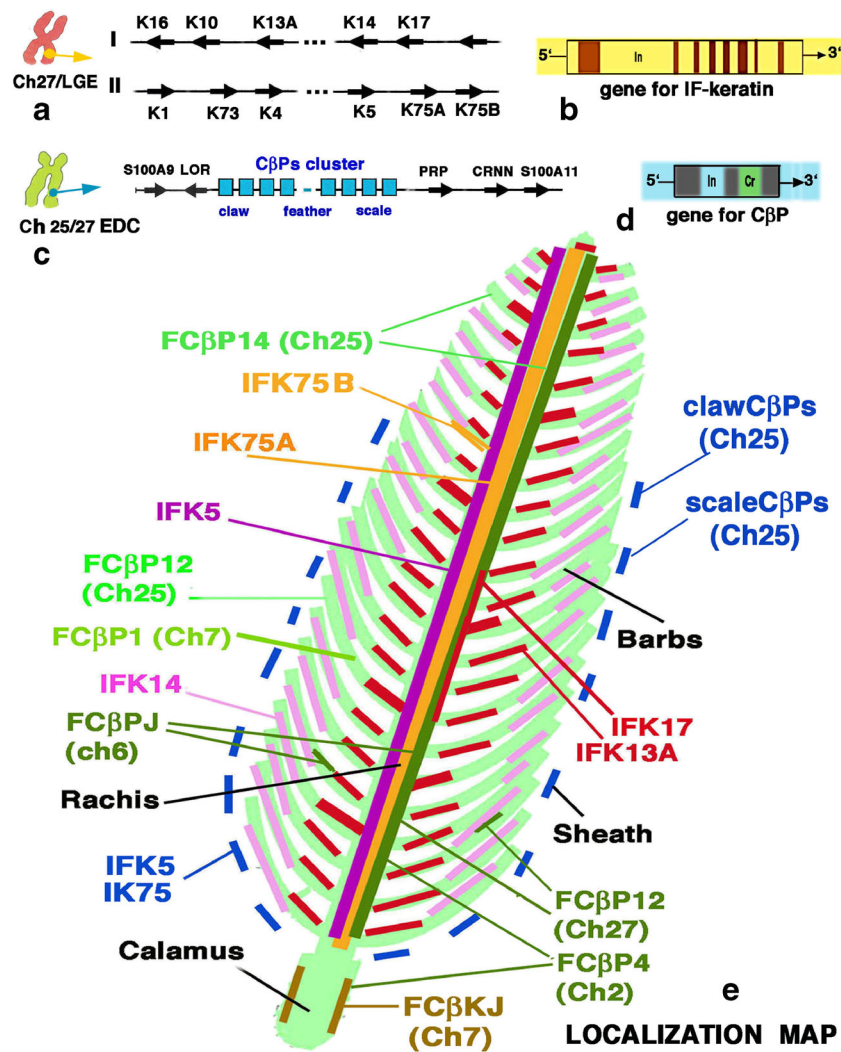
Fig. 2 Schematic drawing showing the gene organization of IF keratins (**a**, **b**) and CbetaPs (**c, d**) with an indicative map distribution of the main proteins in a feather (**e**). **a** Chromosome locus for the alpha-keratin type I cluster (the locus for type II can be in the same or in different chromosomes according to the species) with only few genes indicated with their transcriptional directions 5′–3′ (*arrows*). **b** An example of a gene containing eight coding exons (*black*) separated by introns (*In*, pale). **c** Chromosomal locus containing the EDC, where between the S100A9/ loricrin (LOR) and proline-rich protein/cornulin/S100A11 (PRP, CRNN) genes are localized those for the different types of CbetaPs (CβPs cluster comprising in the order from left to right in 5′ to 3′ direction, claw, feather, beak CPs). **d** The gene structure for CbetaPs, consisting in one intron (In, *pale blue*) and two exons (*black*) with the coding region (Cr) only within the second exon. **e** The expression/localization so far determined for IF keratins and different CbetaPs with their specific chromosomes (indicated as feather keratins by Ng et al. 2012, 2015; Greenwold et al. 2014; Wu et al. 2015)

for cells of the calamus or the rachis in plumulaceous (incoherent) or pennaceous (laminar) feathers. In general, few (3–6) similar IF keratins are present in different regions of feather where only their amount varies. IF keratins are more plentiful in the rachis and calamus compared to the barb and barbules. Conversely, the FCbetaPs are much more numerous and more specialized in their localization within feathers, indicating that these proteins play a major role in the biomechanical properties and morphology of the different regions in a feather (Ng et al. 2014). For instance, 13 FCbetaPs genes located in chromosome 25 code for beta-proteins accumulated in softer contour feathers while 13 other genes present in chromosome 2 encode beta-proteins forming the stiffer flight feathers.

In scales, claws, and beaks, the corneous material is made of glycine-rich, stiff, inflexible, and hydrophobic CbetaPs, which aggregate as irregularly orientated microfibrils and impart resistance and hardness (Sawyer et al. 2000). In feathers, the ordered axial orientation of the corneous bundles made of FCbetaPs produce flexibility and resistance to mechanical tensions and vibrations generated during flight (Fraser et al. 1972; Brush 1978). Other proteins of the EDC devoid of a beta-sheet region, such as the HRP (fast protein) and cysteine-rich proteins (Gregg and Rogers 1986; Strasser et al. 2014) are synthesized during barbules and barbs formation. The specific influence of the unique protein associations located in different regions of feathers on the mechanical performance remains to

be more fully analyzed and evaluated. For example, the Young's modulus (an index of stiffness of an elastic material) increases from the base to the tip of the rachis, and also barbs and barbules have a different consistency and likely molecular organization of the FCbetaPs (Bonser and Purslow 1998; Pabisch et al. 2010).

The complex ramification of feathers and the various feather morphotypes that replace feathers during the lifetime of a bird require not only numerous types of beta-proteins but also the presence of morphogenetic process capable of giving rise to the final branching of barbs, namely the formation of barb ridges (Alibardi 2005a, b, 2006a, b; 2009c).

Development of natal downs and barb ridge morphogenesis

Besides previous light microscopic studies (summarized in Lucas and Stettenheim 1972; Spearman and Hardy 1985; Chuong and Widelitz 1999; Maderson and Alibardi 2000), only two ultrastructural studies of differentiating cells within developing feathers (Filsie and Rogers 1961; Matulionis 1970) and one study of regenerating feathers (Bowers and Brumbaugh 1978), were available before 2005. Ultrastructural studies conducted on developing juvenile and adult regenerating feathers in the chick, zebra finch, quail, and ostrich (Alibardi 2005a, b, 2006a, b, c, 2007a, b, c, d, e, 2008, 2009a, b, c, 2010a, b, 2011a, b), described the ultrastructural details of the main differentiating cells that form natal downfeathers, juvenile and adult feathers, such as barb and barbule cells, supportive cells such as those of sheath, calamus, rachis, dermal papilla, pulp, and pulp cups. The latter are a series of corneous chambers formed at the base of the calamus during the last period of feather growth (Maderson and Alibardi 2000; Alibardi 2009a). The translation of these cytological images into three-dimensional representations of the cell distribution within feathers have indicated that it is the morphogenetic origin of the three-dimensional cell structure of barb ridges and its variations (during the Mesozoic) that have allowed the evolution of the large varieties of feathers (Bartels 2003).

Natal downfeathers develop from small conical germs that elongate into filaments surrounded by a thin sheath where the inner epidermis folds into barb ridges (summarized in Lucas and Stettenheim 1972; Figs. 1Sa, 3, 3S, 4Sa). Inside the sheath, which contains embryonic periderm granules, barb ridges or true barbs form axial parallel lines visible from near the tip of the feather filaments to its base (Figs. 1Sa–e, 3a–d2). Barbules represent the thinnest branched filaments stemming from barbs like the branches of a plant branch or ramus (ramus/rami are also the synonyms for barb/barbs). Eventually, the sheath covering the feather filaments breaks open and the separated barbs open up in a downfeather that deploys from a short calamus or rachis (Figs. 1Sf, 3d–e). After the embryonic

feather is shed and replaced by a juvenile feather, the emerging barbs seen underneath the breaking sheath mainly appear attached to an axial rachis (Fig. 1Sg).

Detailed studies on natal downfeathers show that barb ridges (Fig. 4Sa) are initially absent at the filament tip where a circular epithelium is present (Fig. 4Sb). After the folding of this epithelium, apical barb ridges contain barb and barbule cells and supportive cells, the latter divided into cells of the marginal plates (cylindrical cells), and cells located beneath the sheath (barb vane ridge cells, Matulionis 1970). Cytological and ultrastructural studies have described the differentiation and redistribution of supportive cells among barb and barbule cells within feather filaments (Alibardi 2005a, b, 2006a, b; Alibardi et al. 2006). In the very apical barb ridges, large barb cells are formed and mature into corneous barbs while no or few barbules are formed (Fig. 4Sc, e). The resulting structure at maturity is an un-branched barb with no or only short barbules. Toward the basis of the maturing downfeather filament, barb ridges also form barbule cells that in cross-section appear organized as two rows of dark cells forming the barbule plates (Fig. 4Sf–h). Barbule plates represent cross-sectioned barbules at different developmental stages that are seen in a single plane of section, and comprise younger barbule cells, which are external and close to the sheath and more mature cells which are more internal and close to the ramus. The more internal barbule cells of barbule plates merge with the ramus that represents the branching point of barbules in the mature feather (see the three-dimensional reconstruction of a barb ridge in Fig. 3,b1).

The final branching of feathers occurs through the degeneration of supportive cells which leaves empty spaces among the barbules (Figs. 4Sm 3b2). This process can be best appreciated in longitudinal sections where the barbules appear separated from one another by paler supportive cells (Fig. 4Si–l). The degeneration process occurs after the penetration of the supportive cells among the chains of barbule cells, as this was observed by detailed ultrastructural studies (Alibardi 2005a, b; Fig. 3b1–2). The molecular mechanism responsible for the segregation between barbule and supportive cells is unknown, although different adherens and tight junctions are involved (Chuong and Edelman 1985a, b; Alibardi 2010b, 2011b). The basal retraction of blood vessels and of the mesenchyme inside the feather filament as well as the terminal differentiation of the supportive cells (lipidization and necrosis), of barb cells (lipidization, necrosis and cornification), and of barbule cells (cornification), determines the typical branching of mature feathers (Figs. 4Sm, 3b2).

The main features of downfeather morphogenesis are schematically shown in a simplified form in Fig. 3 which summarizes a generalized image of the collar at the base of the feather filament, viewed across a sheath assumed to be transparent for explanative purposes. Within barb ridges, cells
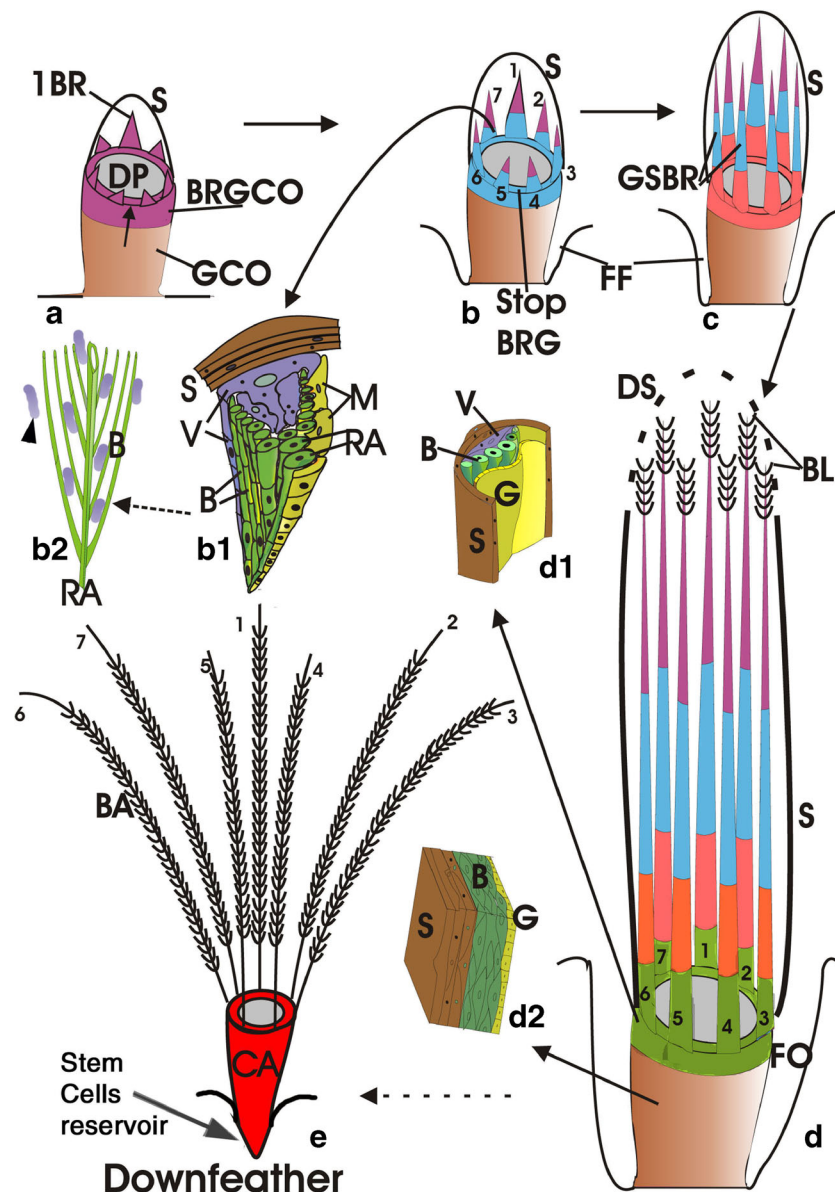
Fig. 3 Drawing featuring the morphogenesis of a downfeather as observed through an ideally transparent sheath. Inside the upper part of the feather germ (*arrow,* **a**) the epidermis forms barb ridges all along the epithelium. The *purple color* indicates that a number of cells are present at a certain time. In a following period more cells are added (indicated in blue color) while old barb ridges have grown longer (**b**). In each barb ridge, the cells organize in a central ramus and lateral barbule columns (*b1*). The cells shown in this sectioned barb ridge are well differentiated and the union between all the chains of barbules cells and the ramus is completed so that the basic feather branching is visible. The next cells produced in the collar and barb ridges (in *red color*) further elongate and separate barb ridges (**c**) which form barbule branching starting from their apical part (**d**) while new cells are added at the base of long barbs (*green color,* **d**). *d1* Details in the folding of the inner epidermis of the feather filament (*yellow*) and the organization of subperiderm cells (*green*) into barb and barbule cells

(*b1*). The cornification of barb and barbule cells and the degeneration of supportive cells (*arrowheads, b2*) transform the barb ridge into a ramus and lateral barbules (*b2*). When no other cells are added to barb ridges at the end of the growth phase, the embryonic epidermis located at the base of the downfeather remains linear as subperiderm layer (*green*) which cells eventually cornify and give rise to the basal calamus (*d2*). Stem cells remain at the base of the follicle (**e**) while the mature and separated barbs (**e**, *1–7* in this example) contain numerous barbules. *B* subperiderm or pre-barb/barbule cells, *BA* mature branched barbs, *BL* branched barbules, *BR* barb ridges (*1BR* first barb ridge), *BRGCO* barb ridge germinal collar, *DP* dermal papilla, *DS* degenerating sheath, *FF* forming feather follicle, *FO* follicle, *G* germinal epithelium, *GCO* germinal epithelium of the collar, *GSBR* growing separated barb ridges, *M* marginal plate cells, *RA* ramus, *S* sheath, *stopBRG* stop in forming barb ridges, *V* barb vane ridge cells (supportive cells)

of the embryonic epidermis are displaced to form two barbule plates and a central ramus area from which the branched shape of barbs is formed (Fig. 3a–b1, d1). The branched appearance of barb ridges results from the insertion of supportive cells

located among barbule cells (violet color in Fig. 3b1, d1) which degenerate leaving separate barbules.

Barb ridges are delimited from the central connective tissue of the feather filament (the pulp) by epithelial cells that form

the marginal plates (yellow color in Fig. 3b1, d1, 2; see Matulionis 1970; Chuong and Widelitz 1999; Alibardi 2005a, b, 2006c, 2007b). At the base of the developing natal downfeather a cylindrical epithelium (the collar) sinks inside the dermis forming a follicle that stores stem cells for the regeneration of the following feather (Chodankar et al. 2002; Fig. 3d, e). After barbs have reached a specific length, the germinal collar stops forming barb ridges so that a circular epithelium reappears while the downfeather enters in a resting stage (telogen) before being replaced from the next feather (termed juvenile feather). Figure 3d, e represents a simple, idealized type of downfeather in which all barb ridges remain separated and terminate on the calamus. In the case of other natal downfeathers in which barb ridges merge at their base, a short rachis is formed instead (Lucas and Stettenheim 1972). The calamus derives from the epithelium of the cylindrical collar after barb ridges are no longer produced (Maderson et al. 2009; Alibardi 2008). The calamus follows the end of formation of barb ridges in the follicle so that the subperiderm layer (the layer accumulating CFbetaPs, green cells in 3b1, d1) remains confined in the upper part of the collar (Alibardi 2002, 2007d). The epithelium of the collar surrounding the retracting pulp at the base of the follicle of downfeathers has not been studied in detail (Lucas and Stetteheim 1972).

The accumulation of FCbetaPs (feather keratins) and another EDC protein rich in cysteine are detected in the subperiderm layer of the embryonic epidermis in alligator and avian epidermis (Fig. 5Sa, b, f, g), but these proteins are predominant in developing feathers (Fig. 5Sc–e, h; Sawyer et al. 2003, 2005; Alibardi 2005b; Strasser et al. 2014). The latter studies have hypothesized that the small FCbetaPs and the cysteine-rich protein present in the subperiderm also continues to be synthesized in barb and barbule cells of avian feathers that are believed to be an elaboration of the subperiderm layer after the evolution of barb ridges.

Feather regeneration and rachis formation

The re-activation of stem cells located in the bulge area of the feather follicle before molting, gives rise to amplifying cells from which new barb ridges and the sheath are formed (Lin et al. 2006, 2013; Yue et al. 2006; Fig. 4a, b). This is a modified recapitulation of the embryonic process of morphogenesis, as it is indicated not only from the renewed synthesis of FCbetaPs, but also from the re-formation of (embryonic) periderm granules in the sheath and supportive cells of regenerating feathers (Kuraitis and Bowers 1978; Alibardi 2006b, 2007b, c). The passage from a circular collar to a folded epithelium where new barb ridges are produced indicates that the three-dimensional shape of different feathers derives from the

induction of barb ridges (see later chapters on dermal papilla and signaling factors).

The labeling with 5-Bromo-2′deoxyuridine (a metabolite incorporated into newly formed DNA, indicating cell duplication), has identified stem cells as long-labeling retaining cells present in the collar, especially located in the bulge region but also in the dermal papilla (Lin et al. 2006; Yue et al. 2005; Alibardi et al. 2014; Fig. 4a–c). These small cells possess few organelles and free ribosomes; their nuclei are mainly euchromatic while their cell surface possess microvilli or folds indicating cell motility (Fig. 4d–f). The re-activation of stem cells derives from poorly known signaling factors likely released from the fibroblasts of the dermal papilla, and these stem cells proliferate and eventually give rise to pennaceous feathers of various types (Lucas and Stettenheim 1972; Spearman and Hardy 1985; Bartels 2003; Chernova 2005, see later in the "Feather regeneration and rachis formation" section).

The histological and ultrastructural study of the follicle in regenerating feathers has shown that the pattern of barb ridge formation in the ramogenic collar, the region where barb ridges are formed, gives rise to different feather morphotypes (Figs. 5, 6, 7, 8, and 9, 6S). The regenerating feather undergoes a growth phase, termed anagen, that is followed by a telogen (resting), and catagen phase (destructive), when the old feather is eliminated from the follicle and replaced by a new feather (Spearman and Hardy 1985). Like in natal downfeathers, the fibroblasts contacting the collar epithelium in the ramogenic region of regenerating feathers penetrate between barb ridges, establishing close contacts with epithelial cells (Alibardi 2005a, 2007a, 2011a; Figs. 6S, 7Sa–g. In contrast to natal downfeathers, barb ridges in regenerating feathers show a more or less pronounced gradation in development, starting from a ventral (posterior) locus where barb ridges appear more immature in cross-section, to a dorsal (anterior) locus where they mature and a rachis is formed (Fig. 6Sa–e). Detailed histological and ultrastructural studies (Alibardi 2005a, b, 2006a, b, 2007a, b, 2008; 2009a, b, c), have indicated that barb ridges vary in length and size in relation to the final length of barbs and barbules and that the apparent position of the ventral locus along the perimeter of the follicle is related to the formation of symmetric and asymmetric feathers (Prum 1999; Prum and Williamson 2001; Alibardi 2009b).

The production of numerous barb ridges in the follicle gives rise to pennaceous feathers with numerous barbs and barbules attached to a rachis (Figs. 5, 6Sa–e), whereas a decrease in the number of barb ridges in the follicle determines the formation of feathers with few and spaced barbs and barbules, such as in bristles and in filoplumes (Figs. 6Sf, g, 6, 7, 8, and 9). These observations have lead to the drafting of drawings that translate the two-dimensional pattern of barb ridge formation into a three-dimensional representation of various morphotypes of feathers (Alibardi 2009b; Figs. 6, 7, 8, and 9). These drawings represent a generalization of the hundreds of different feather

Fig. 4 Schematic presentation (**a**), light (**b**, **c**) and electron microscopy (**d–g**) of chick feather follicle. **a** Base of the follicle which indicated the bulge where stem cells are located. The curved arrows on the *blue-colored* collar indicate possible migration pathways of stem cells. **b** Toluidine blue stain of collar epithelium, bulge, and dermal papilla, oriented as in the previous figure (**a**). *Bar* 25 μm. **c** Detail on the bulge region (*dashes* separate the collar from the dermal papilla) showing the 5BrdU-labeled cells (*arrow*). The orientation is as in the previous figures (**a**, **b**). *Bar* 10 μm. **d** Low electron microscope magnification of small euchromatic cells (*asterisks*) present in the collar epithelium. *Bar* 1 μm. **e** 5BrdU-labeled nucleus of a stem cell localized in the bulge region (silver intensification of the gold-immunolabeled nucleus). *Bar* 0.5 μm. **f** Detail of a small cell with irregular surface (*arrows*) located in the collar epithelium. *Bar* 1 μm. **g** A dermal fibroblast inserting cytoplasmic elongation (*asterisks*) between two barb ridges. *Arrows* indicate melanosomes. *Bar* 1.5 μm. *br* barb ridge, *bu* bulge, *cl* collar epithelium, *de* dermal cell, *dp* dermal papilla, *f* follicle, *it* intermediate differentiating epithelium, *nu* nucleus, *pu* pulp, *rm* ramogenic collar, *sh* sheath
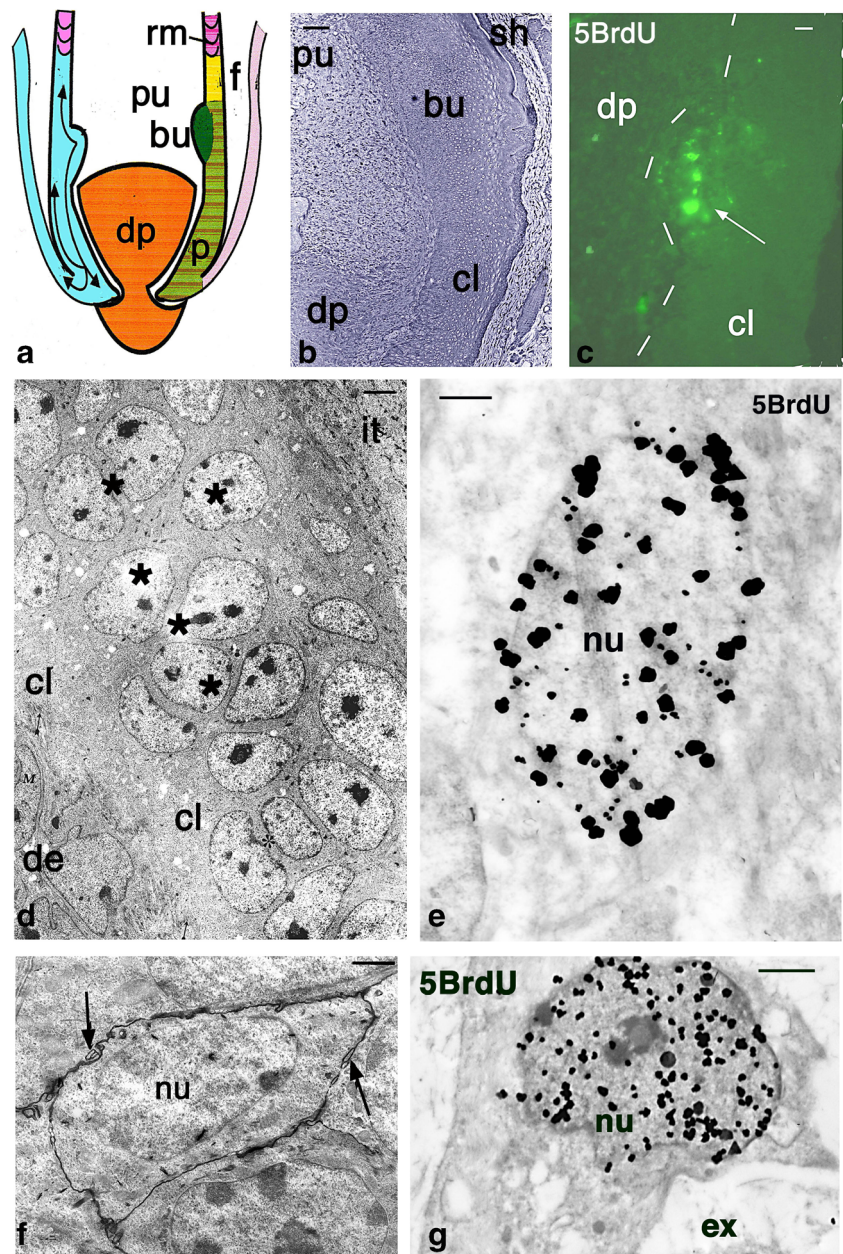
morphotypes that can be generated in different birds, but give an indication on the morphogenetic process that can produce the branching pattern in other morphotypes (Lucas and Stettenheim 1972; Spearman and Hardy 1985; Bartels 2003; Maderson et al. 2009).

In both natal and adult downfeathers and pennaceous feathers, barb ridges grow perpendicular to the ramogenic plane by the addition of new cells from the collar (Figs. 3a–d, 6a, a1). Like in natal downfeathers also in regenerating feathers barb ridges have a similar three-dimensional organization, despite their larger size and number of barbules that elongate the barbule plates (see details in Alibardi 2005a, 2006a, 2007b; compare Figs. 3b1 with 5b). When the direction of growth of

barb ridges occurs in a tilted plane with the ring-shaped bulge (the disc shown in Fig. 5c), this geometrical variation determines the fusion of barb ridges in a point of the collar (considered anterior or dorsal) where barb ridges terminate their identity as separated columns of cells and form the rachis (Fig. 5c–c3). The axial growth of the rachidial ridge lifts up the branched region between rachis and barbs so that a planar feather vane is eventually formed when, later, the feather sheath brakes open (Prum 1999; Prum and Williamson 2001; Alibardi 2008, 2009b; Fig. 5c2–3). The molecular mechanism that determine the tilt of the ramogenic plane, connected with the position of stem cells in the bulge plane, is not known (Yue et al. 2005, but see the section on the dermal papilla and signaling factors).
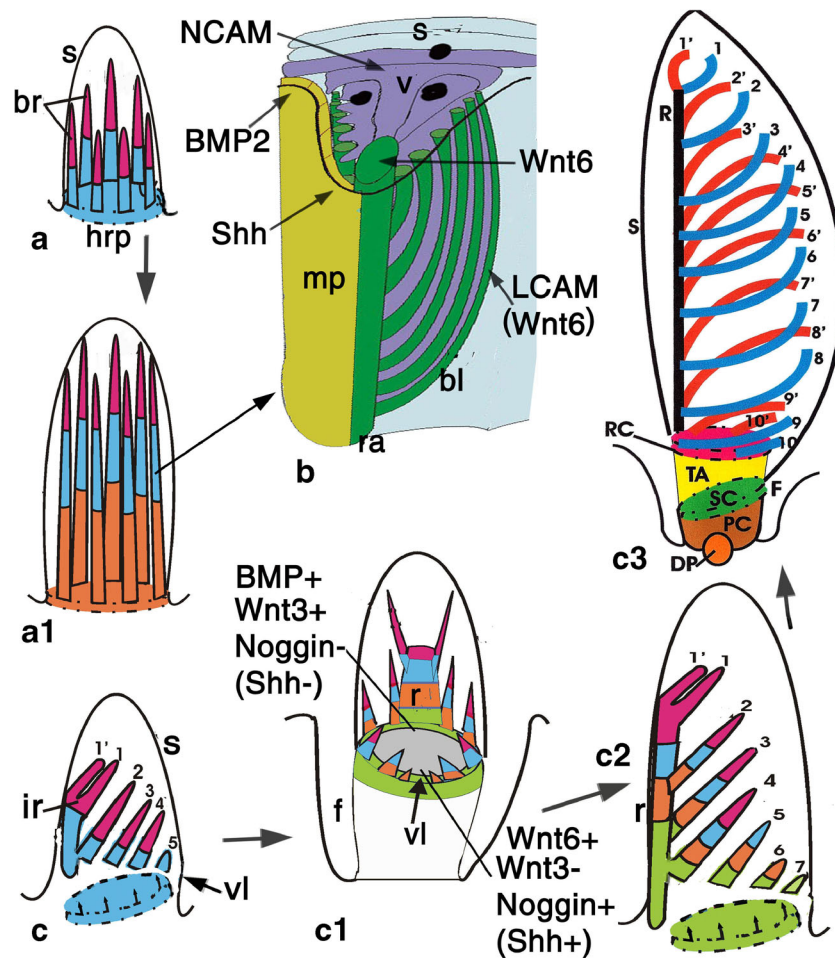
Fig. 5 Morphogenetic process taking place during the formation of downfeathers (**a–a1**), barb ridge with main areas of signaling expression indicated by *arrows* (**b**, see text), and pennaceous feather with numbered rami (**c–c3**, *1–10*). *Different colors* indicate groups of cells generated at progressive periods of feather growth and conserved in their growth into elongating barb ridges and the rachis (*purple* first, then *blue*, *orange*, and *green*, see the text). **a–a1** The barb ridges growing parallel one to another from a horizontal ring-shaped stem cell plane remain separated. **b** Detail of a barb ridge which indicated the higher expression regions (*arrows*) of different gene products (Shh, NCAM etc., see text). **c** The beginning of barb fusion after the stem cell plane has become tilted (only the foreground barb ridges are shown). **c1** Frontal view of a growing feather where a rachis and few barbs are seen with indicated the point of high (+) and low (−) expression of different signaling molecules (see text). **c2** More barb ridges in a growing feather observed from the side. **c3** Further stage where barb ridges are still curved inside the sheath. The collar (the *upper part* containing the proliferating cells derived from stem cells in the bulge (amplifying cells) is shown in *yellow*; the *lower* or papillary part is in *brown*) contains the tilted ring-shaped plane (*green*) where stem cells are located. *bl* barbules, *br* barb ridges, *BMP* bone morphogenetic protein, *dp* dermal papilla, *f* follicle, *hrp* horizontal ramogenic plane, *ir* initial rachis formation, *L-CAM* liver cell adhesion molecule, *mp* marginal plates (made of cylindrical supportive cells), *N-CAM* neural-cell adhesion molecule, *PC* lower part of the collar indicated as papillary collar, *r* rachis, *ra* ramus, *s* sheath, *sc* stem cell plane (bulge), *Shh* sonic hedgehog, *trp* tilted ramogenic plane, *v* barb vane ridge cells (supportive cells), *TA* upper part of the collar occupied by transit amplifying cells that are the cells in rapid proliferation derived from the stem cells plane, *vl* ventral locus, *Wnt* wingless integrated gene

Different barb ridge patterns give rise to different feather types

From the collar of symmetric contour feathers and smaller semiplumes (downfeathers with a short rachis), a series of barb ridges are formed in the anterior part of the follicle, the ventral locus (arrows pointing the collar in Fig. 6a, b). The color code of the ramogenic collar (purple in Fig. 6a) indicates cells in the collar and barb ridges that are produced in the initial phase of anagen. The growth of the feather due to the production along the collar of new cell groups (coded in blue color in Fig. 6b), together with the elongation of the initially formed cell groups (purple), determine the fusion of the two closest barb ridges (BR in Fig. 6a) into a rachidial ridge that elongates into a rachis in the dorsal side of the collar (R in Fig. 6b). The rami produced from these merged barb ridges contain a similar number of cells and, therefore, have the same diameter in both the left and right barb ridges, represented by purple tips in Fig. 6b. This, in turn, determines the formation of barbs of the same length on the left and right sides of the
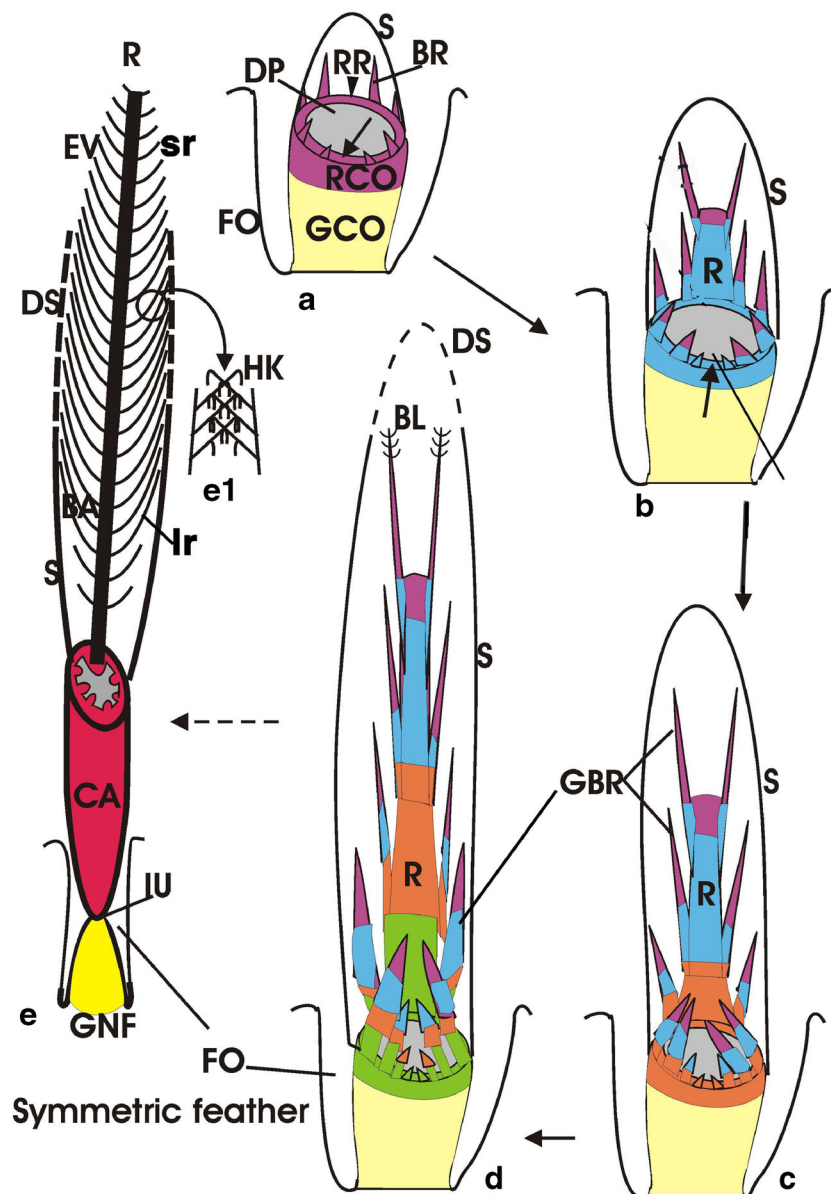
Fig. 6 Schematic drawing illustrating the modality of branching in a symmetric contour feather with a broader vane in the central portion of the feather. Different *colors* indicate groups of cells generated at progressive periods of feather growth and conserved in the elongating barb ridges and the rachis (*purple* first, then *blue, orange,* and *green,* see the text). **a** The ventral locus where new barb ridges of the same size are generated (*arrow*) and the dorsal side where the rachidial ridge is formed after the fusion of the first two barb ridges (*arrowhead*). **b** The initial rachis is now evident. **c, d** The following stages of feather growth. The generation of more barb ridges in following stages (*dotted arrow* between **d** and **e**) give rise to a mature feather which apex remains free from the degenerating sheath (*dashes*, **e**). The feather vane have hooklets that overlap with other barbules to form a close vane (detail in **e1**). *BA* barbs, *BL* barbule, *BR* barb ridge, *CA* calamus, *DG* degenerating sheath, *DP* dermal papilla, *DS* degenerating sheath (*dashes*) *EV* emerging vane, *FO* follicle, *GBR* growing barb ridges, *GCO* germinal collar, *GNF* germ of the next feather, *HK* hooklets, *IU* inferior umbilicus basal-most part of the calamus where the feather will detach from the next generated feather), *MP* marginal plate, *R* rachis, *RA* ramus, *RCO* ramogenic collar, *RR* rachidial ridge, *S* sheath, *V* barb vane ridge cell (supportive cell)

rachis. This process is repeated a number of times (see the sequence of colors, blue, orange and green, Fig. 6 b–d) giving eventually rise to symmetric feathers (Fig. 6e).

Each growing barb ridge (GBR in Fig. 6c, d) undergoes maturation with the formation of piles of barbule cells starting from the tip of the feather and reaching the forming axial ramus at a lower level of the feather where a branching point

is eventually formed (Figs. 5b, 6b–d). While the initial, symmetric barb ridges possess a short ramus (sr in Fig. 6e), barb ridges produced in later stages possess a progressively longer ramus (lr in Fig. 6e) that determines the variation of the width and shape of the feather vane (Fig. 6e). The last barb ridges formed in the follicle, however, progressively reduce the length of their rami and the vane at the base of the rachis
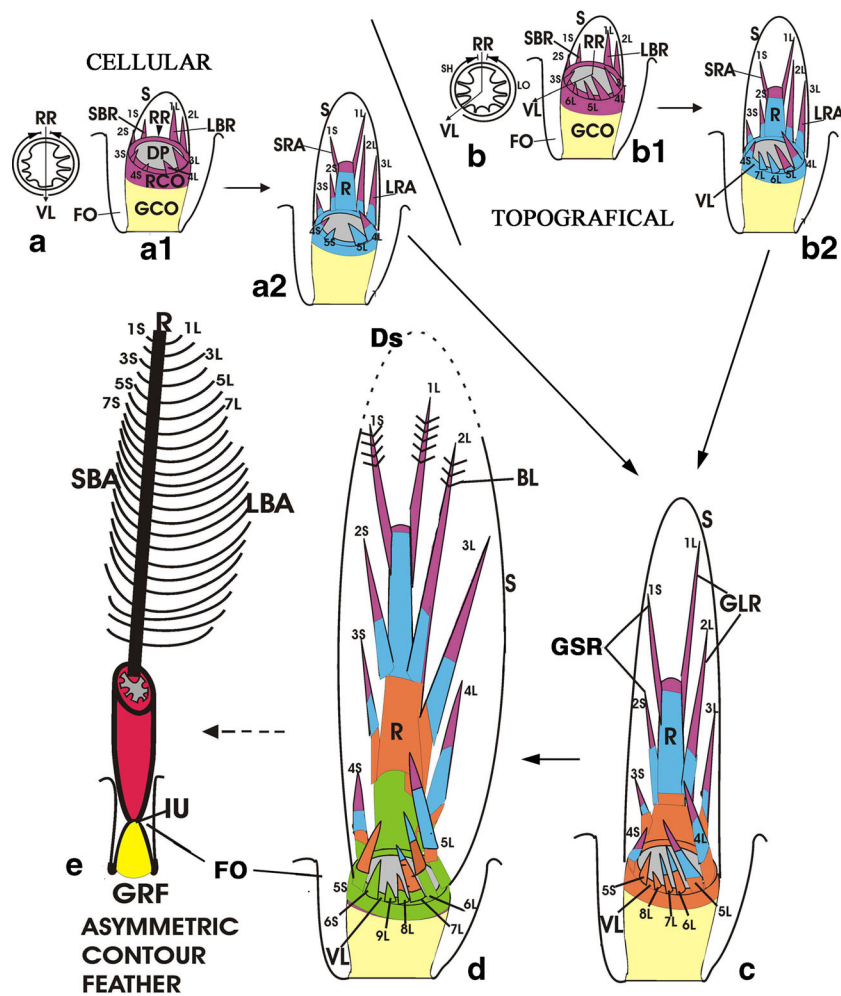
Fig. 7 Schematic representation of stages of morphogenesis in an asymmetric contour feather according to the cellular hypothesis (**a–a2**, see text) and the topographical hypothesis (**b–b2**, see text). Different *color codes* represent groups of cells generated in the collar at progressive periods of growth (anagen) and their following location in the growing feather (first cells formed are colored in *purple*, then in *blue*, *orange*, and *green*). **a** The *arrowhead* indicates the site of formation of the rachidial ridge which is opposite to the ventral locus. **a1** A cross-section of the follicle showing that the curved arrow on the right of the ventral locus has the same length than the curved arrow on the left. **a1–2, c, d** Illustrated progressive phases of growth. Note in *1L–7L* (*L* longer barb ridge) that the size of right barb ridges is bigger and the ramus is longer then the size of the ramus on the left barb ridges indicated as *1S–7S* (*S* shorter barb ridge). The relative growth of the rachis and asymmetric barb ridges in the following stages (*dotted arrow*) gives rise to the mature, asymmetric feather (**e**). **b** A cross-section of the follicle showing that the *curved arrow* on the right of the ventral locus is longer than the *curved arrow* on the left. The curved arrows describe the length of the apparent "helicoidal growth" of barb ridges. **b1–2, c, d** The next three stages of barb ridge formation are shown. Note in *1L–7L* that right barb ridges are longer (*L* longer barb ridges) than left barb ridges indicated as *1S–7S* (*S* shorter barb ridges). The relative growth of the rachis and asymmetric barb ridges in the following stages (*dotted arrow*) produces the mature, asymmetric feather (**e**). *BL* barbula, *BR* barb ridge, *CA* calamus, *DP* dermal papilla, *DS* degenerating sheath (*dotted*), *EV* emerging vane, *FO* follicle, *GCO* germinal collar, *GLR* growing longer ramus, *GRF* germ of the next, regenerating feather, *GSR* growing shorter ramus, *IU* inferior umbilicus, *LBA* longer barbs, *LRA* longer ramus in the barb, *LBR* longer barb ridges, *R* rachis, *RCO* ramogenic collar, *RR* rachidial ridge, *S* sheath, *SBA* shorter barbs, *SBR* shorter barb ridges, *SRA* shorter ramus in the barb

before they disappear forming the calamus (CA in Fig. 6e). The presence of hooklets at the extremities of barbules gives rise to a stabilized velcro-like texture and the formation of a resistant vane (Fig. 6e1). As a result, the feather is narrow at the apex and becomes more expanded in the lower and mid-level of the feather, and narrows again in the lowermost part of the feather before the calamus is formed. The molecular control of the ramus length at different levels of the feather, and of the number and size of barb ridges produced from the collar remains to be discovered.

In asymmetric feathers (coverts, remiges, and rectrices), longer barbs are formed on one side of the rachis (Fig. 7a–e). The length of barbules is probably similar in barbs of both sides of the rachis, and they eventually form a close vane. Therefore, it is the length of the right versus the left ramus that is responsible for this asymmetry. Two possible morphogenetic mechanisms, one cellular (Fig. 7a–a2) and the other topographical (Fig. 7b–b2), can explain the origin of the feather asymmetry (Prum 1999; Prum and Williamson 2001; Alibardi 2009b, c). The cellular mechanism suggests that the

Fig. 8 Schematic representation of the stages of morphogenesis for a filopluma. Different *color codes* represent groups of cells generated in the collar at progressive periods of growth (anagen) and their following location in the growing feather (*purple, blue, orange,* and *green* colors). Only four, right and left, barb ridges are shown in this example (*1–4*) during the elongation of the filoplume (**a–e**). **b** No more barb ridges are formed in the ventral locus so that no more barbs are generated and only a rachis forms (**e**). This process continues in the following stages (*dotted arrow* between **e** and **f**) that produce the final filoplume feather (**f**). The latter only contains the initial four barbs in this example. *AB* apical barbs, *BA* barbs, *BL* barbules, *BR* barb ridges, *BRG* barb ridge generation, *DP* dermal papilla, *DS* degenerating sheath, *FO* follicle, *GBR* growing barb ridges, *GCO* germinal collar, *GRF* new germ of the next regenerating feather, *IU* inferior umbilicus, *NR* naked rachis, *R* rachis, *RR* rachidial ridge, *RCO* ramogenic collar, *S* sheath
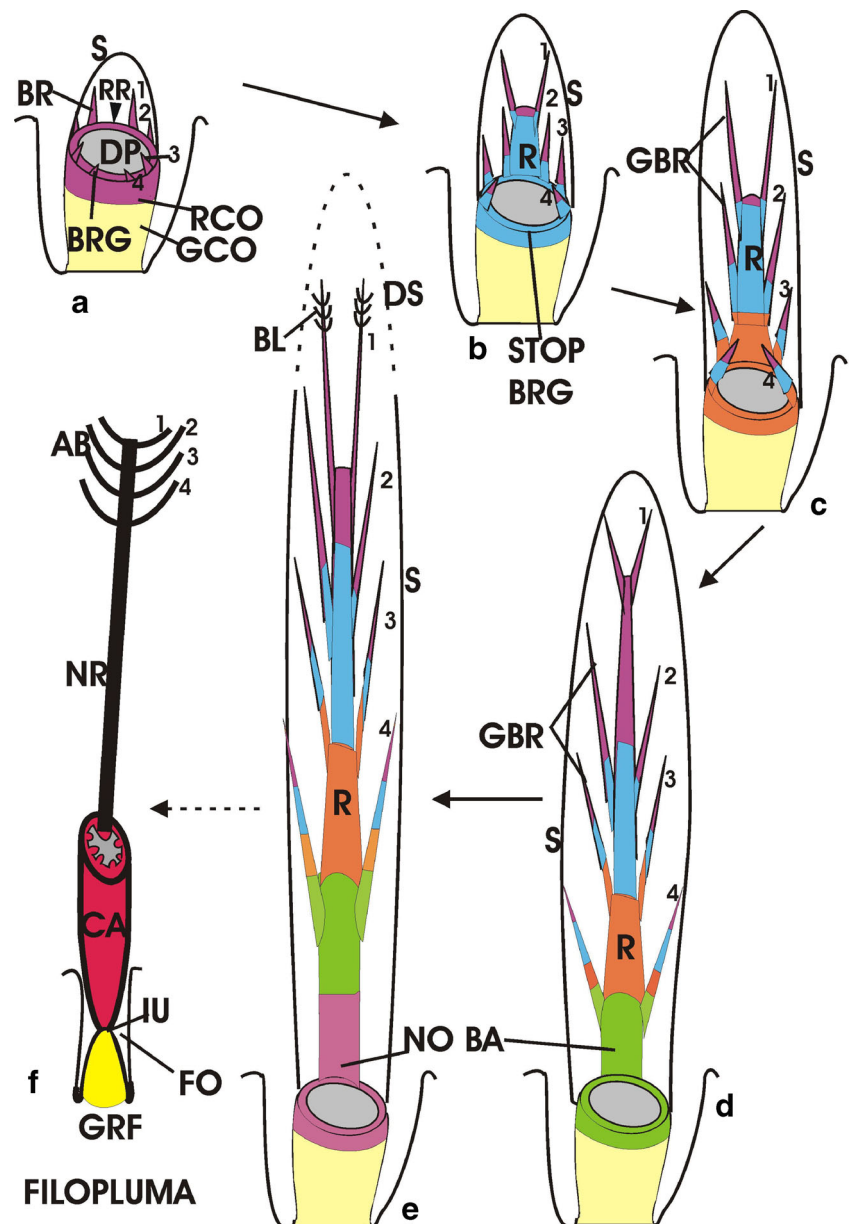
ventral locus (the point of separation between left and right barbs inserting in the rachis) remains in its ventral (posterior) position along the collar, and that it is the number of cells incorporated in a barb ridge or the elongation of cells within each ramus that determine the final length of the ramus. In Fig. 7a1, the right barb ridges (LBR in purple with respect to the rachidial ridge indicated as RR) become longer (not necessarily larger) than the shorter left barb ridges (SBR). From the ventral locus in the collar, longer rami are generated on the right side with respect to the shorter rami produced on the left side (Fig. 7a–a2, b–d), eventually forming the asymmetric feather (Fig. 7e). The constant position of the ventral locus in some asymmetric feathers has been described in zebra finch, chick, and quail feathers (Alibardi 2009a, b). The molecular

mechanisms that determine the control of the cells that are recruited into rami or their elongation responsible for the final length of the ramus with the consequent barb asymmetry are not known.

The topographical mechanism explaining the production of longer rami on one side of the follicle instead derives from a process called "helical growth" (Prum and Williamson 2001; Alibardi 2009b). According to this mechanism, the ventral locus from which new barb ridges are generated, changes its position along the collar, in our example it moves to the left (Fig. 7 VL in b–b2). Therefore, all the newly generated barb ridges on the right side will grow for a longer distance along the curved wall of the follicle (helical growth, see curves along the collar in Fig. 7b) to reach the rachidial ridge located in the

Fig. 9 Schematic drawing on the stages of morphogenesis of a bristle feather. Different *color codes* represent groups of cells generated in the collar at progressive periods of growth (anagen) and their following location in the growing feather (*purple* first, then *blue, orange,* and *green*). No barb ridges (or barb ridges merge immediately into a rachis) are generated in the ventral locus (**a**) and the collar epithelium remains unfolded (**a–b**). **c** A first pair of barb ridges is produced in the ventral locus (numbered as *1*). **d, e** The production of more barb ridges continues so that more barbs are generated (numbered as *2–3*). In the following stages (*dotted arrow* between **e** and **f**) at the base of the final bristle only three barbs are shown (in the example shown in **f**). *BA* barbs, *BB* basal barbs, *BRG* barb ridge generation, *CA* calamus, *DP* dermal papilla, *DS* degenerating sheath, *FBA* forming barbs, *FO* follicle, *GCO* germinal collar, *GRF* new germ of the next regenerating feather, *IU* inferior umbilicus, *NR* naked rachis, *R* rachis, *RR* rachidial ridge, *RCO* ramogenic collar, *S* sheath
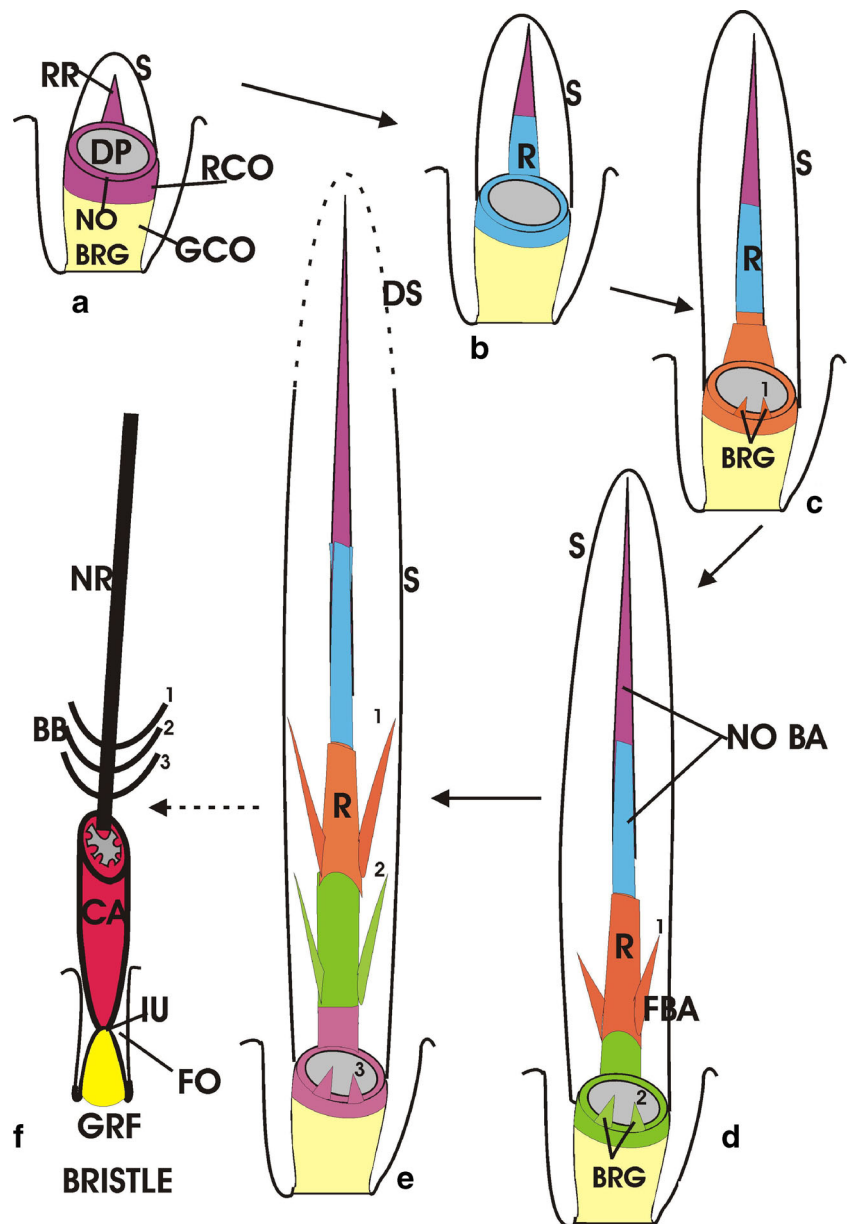
anterior (dorsal) side. The process results in the production of longer rami in the right side of the follicle (Fig. 7b1–d). In our example, at maturity, the right barbs will, therefore, be longer than the barbs located on the left side of the mature feather (Fig. 7e). The variations in the diameter of the papilla and collar (not represented here, see Spearman and Hardy 1985; Alibardi 2005a, details are shown in Alibardi 2009b, c) will also affect the length of barbs. In this figure, the length of formed barbs determines the wider span of the feather vane (LBA in Fig. 7e) during mid anagen, and their decrease in length by the end of anagen, before the calamus is formed. The rate of production of barb ridges on the left side can be higher in comparison to the rate on the right side in order to form a final symmetric branching in the rachis (Prum and

Williamson 2001). The left or right displacement of the ventral locus can be observed in the follicle of some asymmetric feathers in the chick and zebra finch (Alibardi 2008, 2009b). The molecular control that determines the shifting of the ventral locus is not known.

In follicles of filoplumes (Fig. 8 shows a simplified schematic image), some barb ridges are produced at the beginning of anagen (only four barb ridges are represented in Fig. 8a) but their production is rapidly reduced or terminated (Fig. 8b). The hypothesized stop signal to the production of barb ridges from the dermal papilla is unknown in molecular terms. The collar epidermis continues to produce new cells that elongate the rachis without giving rise to further ramifications (barbs; Fig. 8c–e). Continuing the complete or partial absence of barb

ridges production (Alibardi 2008, 2009b, and unpublished observations), the elongating and un-branched rachis forms a filoplume in which only the tufts of apical barbs originally formed are present (four barbs are represented in Fig. 8f).

In another type of small feathers, the bristles (Fig. 9 shows a simplified schematic image), few or no barb ridges are generated at the beginning of anagen, and only the rachidial ridge grows (Fig. 9a, b; Alibardi 2008, 2009b, and unpublished observations). This process of growth determines the formation of an almost naked rachis of variable length. Only later, the collar becomes ramogenic and the first barb ridges are produced from the ventral locus (Fig. 9c–e). The hypothesized start signal for the generation of barb ridges remains to be shown in molecular terms. Continuing this process, new barb ridges are generated in the collar during anagen, and the result of this process is that the initially naked rachis now shows a tuft of basal barbs (only three are shown in Fig. 9f).

As previously indicated for downfeathers, the cessation of the formation of barb ridges and the accumulation of corneous beta-proteins in the intermediate layer of the collar which remains circular, determines the formation of the calamus (Alibardi 2007b). The pulp epithelium around the pulp retracts in successive phases forming a number of pulp cups of unclear significance besides their likely role in forming a barrier to water and microbial penetration into the follicle (see more details in Lucas and Stettenheim 1972; Maderson and Alibardi 2000; Alibardi 2009a; Maderson et al. 2009).

The dermal papilla and its role in feather morphogenesis

The formation of feathers with varied shapes and dimension depends on the activation of the epidermis of the collar under the influence of the dermal papilla (Lucas and Stettenheim 1972; Chuong and Widelitz 1999; Chuong et al. 2003; Widelitz et al. 2003; Maderson et al. 2009; Lin et al. 2013; DiPoi and Milinkowitch 2016). The dermal papilla is necessary for the regeneration of feathers, the formation and position of a rachis, the orientation of feathers, and, therefore, the specification of the feather morphotypes such as symmetric or asymmetric contour feathers, bristles, filoplumes, and so forth (Lucas and Stettenheim 1972; Spearman and Hardy 1985; Chuong and Widelitz 1999; Widelitz et al. 2003). It is unknown whether cells of the dermal papilla form specific three-dimensional connections with epithelial cells in some regions of the collar.

The modulation of the proliferative activity and barb ridge production in the ramogenic collar, in conjunction with the variation in diameter and size of the dermal papilla during anagen, affects the size and length of barb ridges. The growth of barb ridges by the addition of new cells from the collar in a horizontal plane forms separate barbs

(Figs. 3a–d, 5a–a1). The dermal influence primarily affects the size, length, and number of barb ridges produced from the ventral side (or locus) of the feather. The dermis also influences other processes in feather morphogenesis, such as providing mechanical and nutritional support to the differentiating and maturing barb and barbule cells.

In anagen, the dermal papilla is formed by a condensation of small fibroblasts located between the lowermost cylindrical (papillar) collar, and their density may vary in different periods of activity (Spearman and Hardy 1985; Matulionis 1970; Alibardi 2011a). During anagen in the ramogenic zone where barb ridges are forming, dermal cells penetrate between the barb ridges and extend their length in order to contact most of the epithelial cells of the marginal plate (Fig. 7S a, g). Three main types of cell connections are formed between fibroblasts and epithelial cells of barb ridges: anchoring junctions, intracellular microvilli, and pinocytotic vescicles, that are formed on the apposing cell membranes (Alibardi 2005a 2007a; 2011a; Fig. 7S). Anchoring filaments were also seen between dermal cells and the matrix epithelium of the hair bulb (Sugiyama et al. 1976), so that fibroblasts in the feather papilla can communicate mechanical tension in addition to chemical signaling to the epithelium of the marginal plates.

Direct cell-cell contacts between mesenchymal and epithelial cells of the collar are seen in the dermal papilla and in the rim of the papilla cells that extend into the ramogenic zone. In the latter, where barb ridges are formed, the density of dermal cells along the epithelium and the dermal-epidermal contacts decreases while mesenchymal cells stretch along marginal plates (Alibardi 2007a). The dermis from the ramogenic zone is composed of loose cells of the pulp that appear as typical fibroblasts with moderately developed rough endoplasmic reticulum and surrounded by loosely arranged collagen fibrils (Alibardi 2011a). The numerous anchoring filaments noticed in the ramogenic region between epidermal cells of barb ridges and mesenchymal cells suggest that dermal-epidermal interactions here reflect a mechanical connection.

Molecules involved in barb ridge and rachis formation

Dermal cells act by diffusible inductors or through cell-cell contacts on the expression of specific signaling molecules in the epithelium of the collar but also fibroblasts express various gene products involved in pattern formation. It is believed that the cyclical activation and inhibition of cells in the dermal papilla influence the activity of the collar epithelium and eventually, the formation of barb ridges (Spearman and Hardy 1985; Lin et al. 2006, 2013). However, the molecular mechanism that translates a protein signal into the morphogenetic process of formation of barb ridges, their specific pattern of formation, and the origin of the specific feather shape remains unknown.

Among other gene products, identified by PCR and in situ localization of their transcripts or by the immunolocalization of their coded proteins, Sonic hedgehog (Shh), bone morphogenetic proteins (BMP-2 and 4), and Wingless integrated-6 (Wnt-6) play a key role for the morphogenesis of feathers (Harris et al. 2002; Chuong et al. 2003; Chodankar et al. 2002; Widelitz et al. 2003; Yu et al. 2002; Yue et al. 2005, 2006; Lin et al. 2006, 2013; Dhouailly 2009).

Shh is expressed at its highest level in the epithelium of marginal plates near the ramus zone of barb ridges and decreases in the cells of the marginal plates located between barb ridges where BMP2 is highly expressed, especially in cells contacting the sheath (see arrows in Fig. 5b that indicates the sites of higher expression). The transcripts from this gene are later associated with the degeneration of marginal plate cells, but the mechanism of degeneration is not known. This expression in part overlaps with that for neural-cell adhesion molecule (N-CAM, Fig. 5b) that is higher in axial plate cells but disappears after the degeneration of marginal and interbarbule supportive cells (Chuong and Edelman 1985a, 1985b). While the loss of barb vane ridge cells (violet in Fig. 5b) allows the formation of the barbule branching, the loss of marginal plate cells and of the sheath (yellow and light blue in Fig. 5b) allows the formation of separate barbs.

BMP2 is also present in differentiating barb/barbule cells in which also higher levels of L-CAM are present (Chuong and Edelman 1985a, b; Fig. 5b). Therefore, the adhesion of barbule cells to form barbule chains that later become separate from supportive cells is somehow correlated with the differentiation of keratinized cells (barb-barbule cells, L-CAM positive) versus lipogenic cells (supportive cells, N-CAM positive) that later degenerate. N-CAM is also present in dermal papilla cells associated with the epithelial cells of the collar and it is also present in the stretched fibroblasts present between barb ridges in the ramogenic zone (Fig. 7Sg), but this protein disappears in pulp cells. It is likely that this adhesion molecule may be involved in cell communication between mesenchymal cells and collar epithelial cells, possibly by cell-cell contacts.

Wnt-6, whose expression is related to cell proliferation and growth, is evenly expressed in the epithelial cells of the germinal collar, from which new cells are added to form barb ridges. In barb ridges, Wnt-6 is particularly expressed in the ramus region where most cell divisions are located for the increase in the dimension of barb ridges (Fig. 5b). This region is considered an initial grow zone for barb ridges (Chodankar et al. 2002; Yu et al. 2004). This pattern, however, shifts at later stages when the growth zones cease to be a proliferation center and become the zone where the ramus forms. Wnt-6 expression remains associated with the differentiating and elongating barbule cells and with the rami (Fig. 5b) and, therefore, with the formation of long barbs in feathers. The above-mentioned studies have indicated that the combined effect of all these molecules is the production of multiple barb ridges with no fusion into a rachis, as it is typical for natal downfeathers.

The formation of pennaceous feathers requires the presence of a gradient with a dorsal-ventral orientation and is connected to the shift of the ring of stem cells from the horizontal plane in natal downfeathers to an oblique plane in pennaceous feathers (Yue et al. 2005; Lin et al. 2006; Fig. 5a, c). The variation in the location of stem cells probably determines a more rapid differentiation for the derived amplifying cells located in the transitional area (TA in Fig. 5c3) of the posterior (ventral) part of the collar. It is in this area along the collar where new barb ridges start to form (the ventral locus), and then elongate along an apparently tilted ramogenic plane to merge in the anterior (dorsal) area of the collar where the rachis is formed (Fig. 5c-c2).

The combined expression of Wnt-6, BMP-2, Shh, and other genes within the dermal papilla and collar (Fig. 5b) somehow creates the dorsal-ventral (anterior-posterior) gradient responsible for the origin of the rachis (Yue et al. 2006; Lin et al. 2013). In regenerating feathers, Wnt-3 gives rise to a gradient along the follicle collar that is absent in natal downfeathers. This molecule is located in the epithelial cells of the collar and in dermal papilla cells, and its higher expression is present in the dorsal (anterior) side of the follicle where the rachis is formed while the lower expression is present in the ventral (posterior) locus where new barb ridges are formed (Yue et al. 2006; Fig. 5c1). The higher expression of Wnt-3 in the dermal cells near the dorsal locus somehow determines the fusion of barb ridges toward the region of its higher concentration, the rachidial ridge. Also BMP-4 and -2, with the highest site of expression in the mesenchyme of the dorsal locus (Fig. 5c1), promote rachis formation and its enlargement favoring barb ridge fusion.

Noggin and Shh are expressed at higher levels in the mesenchyme close to the ventral locus (Fig. 5c1), and these proteins induce barb ridges formation. This pattern of expression persists through most of the anagen phase, when a number of barb ridges are produced. Noggin determines rachis reduction as its experimental over-expression generates multiple and smaller rachises. In symmetric pennaceous feathers (Fig. 6), Wnt-6 may become more concentrated in the germinal collar of the ventral locus, contributing to the continuous supply of cells utilized for the formation of barb ridges (Yue et al. 2005; Lin et al. 2006). The recruitment of cells for barb ridges formation is similar on both sides of the ventral locus so that barb ridges have similar dimension (Fig. 6). Wnt-3 and BMP may be more concentrated in the dorsal (anterior) side of the follicle where the rachis is formed (Fig. 5c1).

In case of asymmetrical feathers, longer rami, showed on the right side in Fig. 7, may derive from either the recruitment of more cells from the collar or from an increased cell elongation with respect to the opposite barb ridge. Wnt-6 or other proliferation-related genes may be differentially activated in

the right versus the left side of the collar, and the increased protein production may eventually generate longer barb ridges.

Other molecular mechanisms acting on the temporal variation of the production of barb ridges during anagen may be involved in the production of peculiar feathers, such as filoplumes and bristles. Whereas in most anagen of asymmetrical feathers, the molecular gradients (Wnt-3 and BMP versus Noggin, Fig. 5c1) are maintained, the inactivation of these gradients may determine the termination of the ramogenic activity and the disappearance of the rachis that is replaced by the formation of a naked rachis or a calamus. In the follicle of filoplumes, the above-mentioned Wnt3-BMP versus Noggin-Shh gradients may be initially present so that a branched rachis is formed. After a certain number of barb ridges have been produced (four schematically indicated in Fig. 8a, b), the dermal papilla cells change their activity and, therefore, the former gradient is altered and no more barb ridges are produced from the collar. The permanence of a rachidial ridge may be favored by an increase of the level of BMP from dermal and collar cells that somehow enhance the fusion of barb ridges into a rachis in the anterior (dorsal) side of the follicle. Otherwise, the complete inhibition of Noggin (and Shh) expression along the collar may determine the absence of barb ridges production from the ventral locus in the remaining anagen period of filoplumes (Fig. 8b–f). Finally, in follicles of bristles, Wnt/Noggin expression may be absent at the beginning of anagen while only BMP may be present along most of the collar. This condition may determine the formation of a large rachis while barb ridges formation is blocked or their fusion into a rachis is very accentuated. This process results in a compact rachis with no ramification during the first part of anagen (Fig. 9a–c). The formation of the typical Wnt-BMP versus Noggin-Shh gradient in a later phase of anagen, controlled by a variation in cell induction from the dermal papilla, may determine the setting of the gradient with an increase in Noggin expression in the ventral locus. This mechanism may give origin to barb ridges from the ventral locus and the formation of barbs in the lower part of the rachis at later phases of anagen (Fig. 9c–f). Despite the above-mentioned information and hypotheses, the translation of the gene expression into the three-dimensional morphogenetic process forming natal downfeathers and various types of pennaceous feathers remains presently unexplained.

Feather evolution and final considerations

Previous hypotheses on feather evolution favor the tubular origin of feathers from conical skin appendages indicated as proto-feathers (Prum 1999; Brush 2000; Chuong et al. 2000; Prum and Brush 2002; O'Connors et al. 2012). The present, general hypothesis illustrated in Fig. 10 is based on the histological and ultrastructural analyses of barb ridge morphogenesis in both downfeathers and regenerating feathers, and emphasizes the role of supportive cells on the morphogenesis of barb ridges as a key feature for the evolution of feathers, especially for the origin of the barbule ramification (see details in Alibardi 2005b, 2006a, 2007b, 2009c; Alibardi and Toni 2008). These ultrastructural and immunocytochemical studies have indicated that supportive and barb/barbule cells derive from the expansion of the second and of the third embryonic layer, respectively, formed in the feather filament (Sawyer et al. 2005; Alibardi 2006b; Alibardi et al. 2006; Strasser et al. 2014; Fig. 3b–d). The present hypothesis considers that the sequence of development of modern feathers recapitulates their progressive steps in evolution, from simple to complex, therefore from feather filaments to downy feathers, and later to pennaceous feathers (Prum and Brush 2002; O'Connors et al. 2012).

Previous hypotheses considered successive stages of feather evolution in terms of a progressive complexity of the branching pattern (stages 2, 3, 4 according to Prum 1999; Brush 2000; Chuong et al. 2000; O'Connors et al. 2012). The present hypothesis instead indicates that barbule branching is not necessarily a successive stage of un-branched barbs but a variation in the pattern of the branching of barb ridges that might have occurred at the same time during evolution. This means that branched stages with numerous barbules (e.g., stages 3–5 according to Prum 1999) are not necessarily successive to less branched stages made only of barbs (stages 2–3 according to Prum 1999). In fact, the formation of branched or un-branched barbs depends on the interactions between supportive and barb/barbule cells, and the pattern of interactions gives rise to different shapes of barb ridges and later of barb ramification (see details in Alibardi 2006a, b; 2009c).

In the Mesozoic archosaurians like theropods, skin derivatives varied from flat to tuberculate scales but also short filaments have been found in the fossil record (Maderson 1972b; Griffihs, 1998; Martin and Czerkas 2000; Sumida and Brochu 2000; Coria and Chiappe 2007; McKellar et al. 2011). We hypothesize here that the number of CbetaPs necessary to make this relatively limited variety of appendages was probably not higher than 20–40, as in lizard (Dalla Valle et al. 2010), or 20–21 as in crocodilians (Greenwold and Sawyer 2013), or 30–40 beta-proteins present in chick scales, claws, and beaks (Figs. 1S, 10, n. 1–5). The plastic genome of avian archosaurs likely underwent dramatic changes when hair-like scale derivations or filamentous appendages evolved in the avian lineage in association with other anatomical features of birds that allowed these archosaurians to evolve homeothermy and later flight (Hillenius and Ruben 2004; Fig. 10, n. 6–7). Over 100 small FCbetaPs of 97–105 amino acids (feather beta-keratins) were produced in the Epidermal Differentiation Complex locus (EDC), in conjunction with the evolution of genes orchestrating the morphogenesis of barb ridges (Fig. 10, n. 8–9). These genes were probably present in the scaled archosaurian
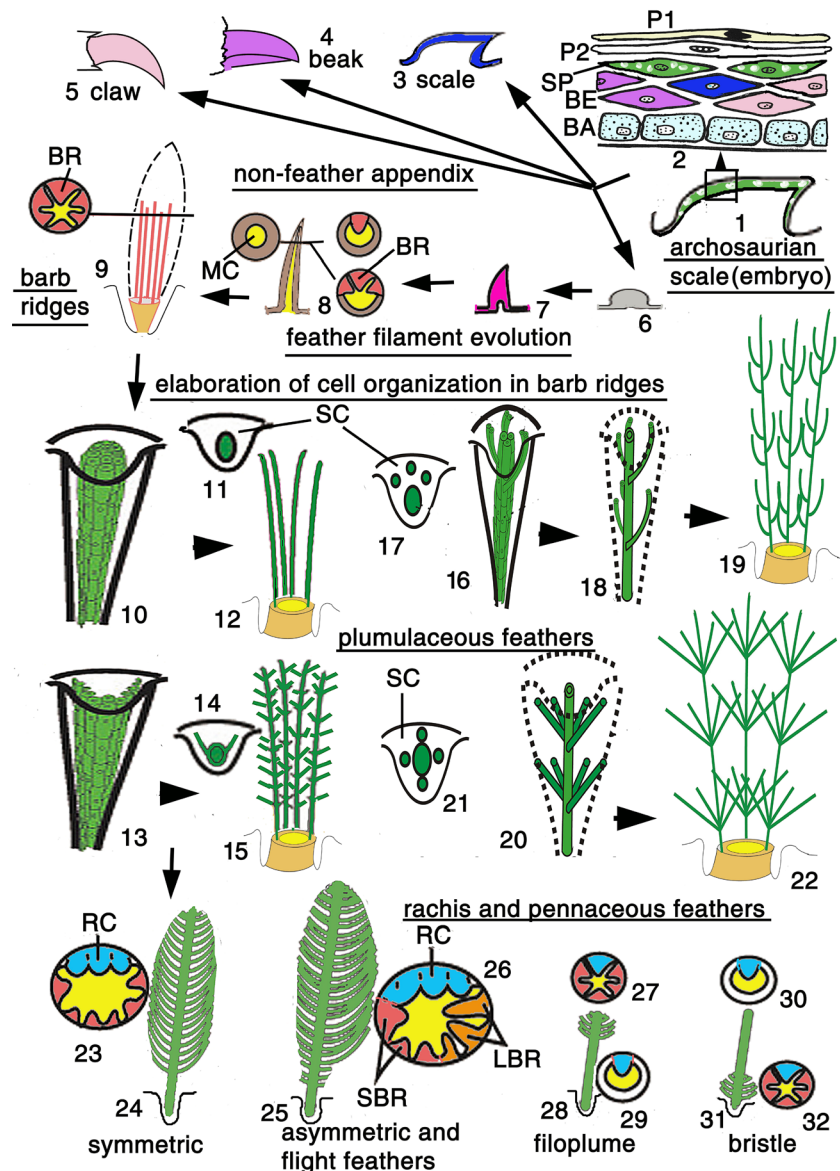
Fig. 10 Schematic representation of feather evolution from a scaled integument of basal archosaurians (*1*). The embryonic epidermis (*2*) can activate genes for scale (*blue*), beak (*purple*), or claw (*pink*) beta-proteins in different regions (*3–5*). From a tuberculate scale (*6*), a cone-shaped appendage without dermal core (*7*) became more elongated and was later colonized by a vascular mesenchymal core (MC in *yellow*, *8*). One or more barb ridges (BR in *red*) were formed producing separate barbs that gave rise to downfeathers (*9*). The further elaboration of a barb ridge (seen frontally in *10* and *13* and *11* and *14* in cross-section) was due to the different three-dimensional association between supportive cells (SC) and barb-barbule cells (in *green*), and produced naked (*12*) and other forms of barb ramification (*10–22*). The hypothetic alternate (*19*) and raceme (*22*) branching is absent in modern barbs, which are mostly symmetric and planar branched (*15*). When barb ridges merged according to different patterns into a rachis (cross-sections in *23*, *26*, *27*, *29*, *30*, *32*), different types of pennaceous feathers evolved. Among others, only the asymmetric type (*25*) allowed flight in conjunction to other characteristics that evolved in birds. *BA* basal epidermis, *BE* suprabasal beta-keratinocytes, *P1* outer periderm, *P2* inner periderm, *RC* rachis, *SP* subperiderm layer

epidermis before feather emerged, but only the shorter feather beta-proteins, devoid of the glycine-rich tail (Fig. 2S, 3S), were used in these filamentous appendages. After the process of barb ridge morphogenesis evolved through the interaction between supportive cells and barb-barbule cells (see details in Alibardi 2005b; 2006 a, b, c; b; 2009c), different cell arrangements and barbule branchings were possibly generated and required more types of FCbetaPs. With the origin of a

calamus, axial rachis, hook barbules, and juvenile and adult feather types (Fig. 10, n. 10–32), the number of genes coding for the specialized beta-proteins of feathers further increased (Fig. 3S). Also other corneous proteins, different from both alpha-keratins and beta-proteins, evolved within the EDC of birds (Vanhoutteghem et al. 2008; Strasser et al. 2014, 2015; Mlitz et al. 2014), but their role in feather cornfication is not known yet. Feathers evolved as peculiar branched horny

appendages from skin tubercles of archosaurian reptiles that covered the integument of theropods and early birds, probably in relation to homeothermy and/or behavioral display (Martin and Czerkas 2000).

The archosaurian scaled integument in which finger tips were modified into claws, initially expressed genes coding for scale, claw, and beak beta-proteins, and these proteins contained long-tail regions rich in glycine-repeats and tyrosines (scale-claws KAbetaPs, Fig. 10, n. 1–5). Perhaps other genes produced also shorter beta-proteins devoid of the tail region and containing a feather epitope, that were used in corneocytes of coniform scales or in elongated cells of piliform appendages (proto-feathers, Fig. 10, n. 6–7).

The piliform appendages became hollowed, and were colonized by the mesenchyme and blood vessels so that a new morphogenetic process forming one or more epidermal folds or barb ridges were established (Fig. 10, n. 8–9; see Alibardi 2009c). It was the innovation and elaboration of the morphogenesis of barb ridges and the origin and redistribution of supportive and feather cells that produced diverse types of barbule branching, from rami with no branches (naked) to complex branches like those found in Mesozoic and modern feathers (Fig. 10, n. 10–22). However, the association between barbule and supportive cells might have created other, uncommon forms of barbule ramifications, such as the alternate (Fig. 10, n. 19) or racemic (Fig. 10, n. 22) barbs, that were likely eliminated by natural selection in favor of the classical types. Therefore, although naked barbs are the simplest structures, also branched barbs could be generated at the same time in evolution by the different association between supportive and barb/barbule cells within barb ridges. Only later, after the ramogenic plane moved from a horizontal to a tilted orientation, barb ridges merged to originate a rachis (Fig. 10, n. 23). Some specialized feathers became planar and were utilized for contour, display, insulation, mechanical protection, and a few types (asymmetric pennaceous) with a planar vane were eventually utilized for flight (Fig. 10, n. 24–32).

Final remarks and future directions

The next studies on feather formation should analyze the specific gene regulation for the rapid production of FCbetaPs (feather keratins), and their polymerization in association with other proteins of the EDC present in feather cells (Calvaresi et al. 2016). The knowledge of the timing and tissue expression of numerous FCbetaP genes would allow to correlate the feather shape with specific proteins that accumulate in the rachis, calamus, and barbs, the basis for understanding the different biomechanical properties of feathers (Bonser and Purslow 1998; Pabisch et al. 2010). However, the mechanism of translation of the messages originated from the dermal papilla and sent to the collar epidermis that activates the

specific pattern of barb ridges formation responsible for producing the enormous variety of feather types, remains the main challenge to be elucidated in feather biology.

Compliance with ethical standards

Conflict of interest   The author declares that there are no competing interests.

References

Alibardi L (2002) Keratinization and lipogenesis in epidermal derivatives of the zebrafinch *Taeniopygia guttata castanotis* (Aves, Passeriformes, Ploceidae) during embryonic development. J Morph 251:294–308

Alibardi L (2004) Dermo-epidermal interactions in reptilian scales: speculations on the evolution of scales, feathers and hairs. J Exp Zool 302B:365–383

Alibardi L (2005a) Fine structure of juvenile feathers of the zebrafinch in relation to the evolution and diversification of pennaceous feathers. J Subm Cytol Path 37:323–343

Alibardi L (2005b) Cell structure of developing barb and barbules in downfeathers of the chick: central role of barb ridge morphogenesis for the evolution of feathers. J Submicr Cytol Path 37:19–41

Alibardi L (2006a) Cells of embryonic and regenerating germinal layers within barb ridges: implication for the development, evolution and diversification of feathers. J Submicr Cytol Path 38:51–76

Alibardi L (2006b) Cell structure of barb ridges in downfeathers and juvenile wing feathers on the developing chick embryo: barb ridge modifications in relation to feather evolution. Ann Anat 188:303–318

Alibardi L (2007a) Cell interactions in barb ridges of developing chick downfeather and the origin of the feather branching. Ital J Zool 74: 143–155

Alibardi L (2007b) Cell organization of barb ridges in regenerating feathers of the quail: implication of the elongation of barb ridges for the evolution and diversification of feathers. Acta Zool 88:101–117

Alibardi L (2007c) Wedge cells during regeneration of juvenile and adult feathers and their role in carving out the branching pattern of barbs. Ann Anat 189:234–242

Alibardi L (2007d) Keratinization of sheath and calamus cells in developing and regenerating feathers. Ann Anat 189:583–595

Alibardi L (2007e) Cytological aspects of the differentiation of barb cells during the formation of the ramus in feathers. Int J Morphol 25:73–83

Alibardi L (2008) Ultrastructure of the feather follicle in relation to the formation of the rachis and pennaceous feathers. Anat Sci Int 85: 79–91

Alibardi L (2009a) Cornification of the pulp epithelium and formation of pulp cups in downfeathers and regenerating feathers. Anat Sci Int 84:269–279

Alibardi L (2009b) Follicular patterns during feather morphogenesis in relation to the formation of asymmetric feathers, filoplumes and bristles. Ital J Zool 76:279–290

Alibardi L (2009c) Molding and carving cell surfaces: the joke of a fold and the origin and evolution of feathers. In: Gorb S (ed) Surface biology. Springer, Heidelberg-London-New York, pp 163–176

Alibardi L (2010a) Cornification of the beak of *Rana dalmatina* tadpoles suggest the presence of basic keratin-associated proteins. Zool Stud 49:51–63

Alibardi L (2010b) Gap and tight junctions in the formation of the feather branches: a descriptive ultrastructural study. Ann Anat 192:251–258

Alibardi L (2011a) Ultrastructure of cells of the dermal papilla in pennaceous feathers. Trends Dev Biol 5:51–60

Alibardi L (2011b) Cell junctions during morphogenesis of feathers: general ultrastructure with emphasis on adherens junctions. Acta Zool 92:89–100

Alibardi L (2013) Immunolocalization of alpha-keratins and feather beta-proteins in feather cells and comparison with the general process of cornification in the skin of mammals. Ann Anat 195:189–198

Alibardi L, Segalla A (2011) The process of cornification in the horny teeth of the lamprey involves proteins in the keratin range and other keratin-associated proteins. Zool Stud 50:416–425

Alibardi L, Toni M. 2006. Cytochemical, biochemical and molecular aspects of the process of keratinization in the epidermis of reptilian scales. Prog. Histoch Cytoch 40: 73-134

Alibardi, L., Toni, M., and Dalla Valle, L., 2007. Hard cornification in reptilian epidermis in comparison to cornification in mammalian epidermis. Experimental Dermatology 16: 961-976

Alibardi L, Toni M (2008) Cytochemical and molecular characteristics of the process of corneification during feather morphogenesis. Progress Histoch Cytoch 43:1–72

Alibardi L, Knapp LW, Sawyer RH (2006) Beta-keratin localization in developing alligator scales and feathers in relation to the development and evolution of feathers. J Submicr Cytol Path 38:175–192

Alibardi L, Dalla Valle L, Nardi A, Toni M (2009) Evolution of hard proteins in the sauropsid integument in relation to the cornification of skin derivatives in amniotes. J Anat 214:560–586

Alibardi L, Wu P, Chuong MC (2014) Ultrastructural characteristics of 5BrdU labeling retention cells including stem cells of regenerating feathers in chicken. J Morphol 275:768–774

Baden, H.P., Maderson, P.F., 1970. Morphological and biophysical identification of fibrous proteins in the amniote epidermis. J. Exp. Zool. 174, 225–232

Barnes GL, Sawyer RH (1995) Histidin-rich protein B of embryonic feathers is present in the transient embryonic layers of scutate scales. J Exp Zool 271:307–314

Bartels T (2003) Variations in the morphology, distribution, and arrangement of feathers in domesticated birds. J Exp Zool B 298:91–108

Bell, E., Thatachari, Y.T., 1963. Development of feather keratin during embryogenesis of the chick. J. Cell Biol. 16, 213-223

Bonser RHC, Purslow PP (1998) The Young's modulus of feather keratin. J Exp Biol 198:1029–1033

Bowers RR, Brumbaugh JA (1978) An ultrastructural study of the regenerating breast feather of the fowl. J Morphol 158:275–290

Bragulla HH, Homberger DG (2009) Structure and functions of keratin proteins in simple, stratified, keratinized and cornified epithelia. J Anat 214:516–559

Brush AH (1978) Feather keratins. In: Brush AH (ed) Chemical zoology, vol X, Academic Press. New York, San Francisco, London, pp 117–140

Brush AH (1983) The origin of feathers: a novel approach. In: Farner D, King JA, Parker KC (eds) Avian biology, vol IX. Academic Press Ltd., New York, pp 121–162

Brush AH (1986) Tissue specific protein heterogeinity in keratin structures. Bioch System Ecol 14:477–551

Brush, A.H. (1993). The origin of feathers: a novel approach. In Farner D, King JA and Parker KC (Eds): Avian Biology IX, pp 121-162. New York: Academic Press

Brush AH (2000) Evolving a protofeather and feather diversity. Amer Zool 40:631–639

Calvaresi M, Eckhart L, Alibardi L (2016) The molecular organization of the beta-sheet region in corneous beta-proteins (beta-keratins) of sauropsids explains its stability and polymerization into filaments. J Struct Biol. Doi: 10.1016/j.Jsb.2016.03.004.

Candi E, Schmidt R, Melino G (2005) The cornified envelope: a model of cell death in the skin. Nature Rev Mol Cell Biol 6:328–339

Chernova OF (2005) Polymorphism of the architectonics of definitive contour feathers. Doklady Biol Sci 405:437–442

Chodankar R, Cheng CH, Yue Z, Jiang X, Suskaweang S, Burrus LW, Chuong CM, Widelitz RB (2002) Shift of localized growth zones contributes to skin appendage morphogenesis: role of the Wnt/β−catenin pathway. J Inv Dermat 120:20–26

Chuong CM, Edelman GM (1985a) Expression of cell-adhesion molecules in embryonic induction I morphogenesis of nestling feathers. J Cell Biol 101:1009–1026

Chuong CM, Edelman GM (1985b) Expression of cell-adhesion molecules in embryonic induction II morphogenesis of adult feathers. J Cell Biol 101:1027–1043

Chuong CM, Widelitz RB (1999) Feather morphogenesis: a model of the formation of epithelial appendages. In: Chuong CM (ed) Molecular basis of epithelial appendage morphogenesis. Landes Bioscience, Georgetown, Texas, USA, pp 57–73

Chuong CM, Chodankar R, Widelitz RB, Jian TX (2000) Evo-devo of feathers and scales: complex epithelial appendages. Curr Opin Gen Dev. 449–456.

Chuong MC, Wu P, Zhang FC, Xu X, Yu M, Widelitz RB, Jiang TX, Hou L (2003) Adaptation to the sky: defining the feather with integument fossils from mesozoic china and experimental evidence from molecular laboratories. J Exp Zool 298B:42–56

Coria RA, Chiappe LM (2007) Embryonic skin from late cretaceous sauropsids (dinosauria) of auca mahuevo, patagonia, Argentina. J Paleont 81:1528–153

Coulombe PA, Omary MB (2002) 'Hard' and 'soft' principles defining the structure, function and regulation of keratin intermediate filaments. Curr Opin Cell Biol 14:110–122

Dalla Valle L, Toffolo V, Belvedere P, Alibardi L (2005) Isolation of a mRNA encoding a glycine-proline-rich beta-keratin expressed in the regenerating epidermis of lizard. Dev Dyn 234:934–947

Dalla Valle L, Nardi A, Toffolo V, Niero C, Toni M, Alibardi L (2007a) Cloning and characterization of scale beta-keratins in the differentiating epidermis of geckos show they are glycine-proline-serine-rich proteins with a central motif homologous to avian beta-keratins. Dev Dyn 236:374–388

Dalla Valle L, Nardi A, Belvedere P, Toni M, Alibardi L (2007b) Beta-keratins of differentiating epidermis of snake comprise glycine-proline-serine-rich proteins with an avian-like gene organization. Dev Dyn 236:1939–1953

Dalla Valle L, Nardi A, Gelmi C, Toni M, Emera D, Alibardi L (2008) Beta-keratins of the crocodilian epidermis: composition, structure, and phylogenetic relationships. J Exp Zool 312B: 42-57

Dalla Valle L, Nardi A, Alibardi L (2009a) Isolation of a new class of cysteine-glycine-proline rich beta-proteins (beta-keratins) and their expression in snake epidermis. J Anat 216:356–367

Dalla Valle L, Nardi A, Gelmi C, Toni M, Alibardi L (2009b) Beta-keratins of the crocodilian epidermis: composition, structure, and phylogenetic relationships. J Exp Zool 312B:42–57

Dalla Valle L, Nardi A, Toni M, Alibardi L (2009c) Beta-keratins of turtle shell comprise small glycine-proline-tyrosine rich proteins similar to those of crocodilians and birds. J Anat 214:284–300

Dalla Valle L, Nardi A, Bonazza G, Zuccal C, Emera D, Alibardi L (2010) Forty keratin-associated β−proteins (β-keratins) form the hard layers of scales, claws and adhesive pads in the green anole lizard, *Anolis carolinensis*. J Exp Zool 314B:11–32

Dhouailly D (2009) A new scenario for the evolutionary origin of hair, feather, and avian scales. J Anat 214:587–606

DiPoi N, Milinkowitch MC (2016) The anatomical placode in reptile scale morphogenesis indicates ancestry among skin appendages in amniotes. Sci Adv 2:e1600708 (1–8)

Filsie BK, Rogers GE (1961) An electron microscope study of the fine structure of feather keratin. J Cell Biol 13:1–12

Fraser RD, Parry DA. 1996. The molecular structure of reptilian keratin. Int J Biol Macromol 19: 207-211

Fraser RD, Parry DA (2008) Molecular packing in the feather keratin filament. J Struct Biol 162:1–13

Fraser RD, Parry DA (2011) The structural basis of the filament-matrix texture in the avian/reptilian group of heard β-keratins. J Struct Biol 173:391–405

Fraser RDB, Macrae TP, Rogers GE (1972) Keratins: their composition, structure and biosynthesis. Charles C. Thomas, , Springfield, IL, USA

Fuchs E, Tyner AL, Giudice GJ, Marchuk D, RayChaudhury A, Rosember M (1987) The human keratin genes and their differential expression. Curr Top Dev Biol 22:5–34

Gillespie JM (1991) The structural proteins of hair: isolation, characterization and regulation of biosynthesis. In: Goldsmith LA (ed) Physiology, biochemistry and molecular biology of the skin. Oxfors University Press, Oxford, pp 625–659

Glenn TC, French JO, Heincelman TJ, Jones KL, Sawyer RH (2008) Evolutionary relationships among species of feather beta (β) keratin genes from several avian orders. Integ Comp Biol 48:463–475

Greenwold MJ, Sawyer RH (2010) Genomic organization and molecular phylogenies of the beta keratin multigene family in the chicken (Gallus gallus) and zebrafinch (Taeniopygia guttata): implications for feather evolution. BioMed Cent Evol Biol 10:148–163

Greenwold MJ, Sawyer RH (2011) Linking the molecular evolution of avian beta keratins to the evolution of feathers. J Exp Zool 316: 609–616

Greenwold MJ, Sawyer RH (2013) Expression of archosaurian beta-keratins: diversification and expansion of archosaurian beta-keratins and the origin of feather beta-keratins. J Exp Zool 320B:393–405

Greenwold MJ, Bao W, Jarvis ED, Hu H, Li C, Gilbert MTP, Zhang G, Sawyer RH (2014) Dynamic evolution of the alpha (α) and beta (β) keratins has accompanied integument diversification and the adaptation of birds into novel lifestyles. BMC Evol Biol 14:249–265

Gregg K, Rogers GE (1986) Feather keratins: composition, structure and biogenesis. In: Bereither-Hahn J, Matoltsy GA, Sylvia-Richards K (eds) Biology of the integument, vertebrates 2. Berlin, Springer-Verlag, New York, pp 666–694

Gregg K, Wilton S, Rogers GE, Molloy PL (1983) Avian keratin genes: organization and evolutionary inter-relationships. In: Nagley P, Linnane AW, Peaock WL, Pateman JA (eds) Manipulation and expression of genes in eucaryotes. Academic, London/New York, pp 65–72

Gregg K, Wilton SD, Parry DA, Rogers GE (1984) A comparison of genomic coding sequences for feather and scale keratins: structural and evolutionary implications. EMBO J 3:175–178

Haake AR, Konig G, Sawyer RH (1984) Avian feather development: relationships between morphogenesis and keratinization. Dev Biol 106:406–413

Harris MP, Fallon JF, Prum RO (2002) Shh-Bmp2 signaling module and the evolutionary origin and diversification of feathers. J Exp Zool 294B:160–176

Hillenius WJ, Ruben JA (2004) The evolution of endothermy in terrestrial vertebrates: who? when? why? Physiol Biochem Zool 77:1019–1042

Holthaus KB, Strasser B, Sipos W, Schmidt HA, Mlitz V, Sukseree S, Weissenbacher A, Tschchler E, Alibardi L, Eckhart L (2015) Comparative genomics identifies epidermal proteins associated with the evolution of the turtle shell. Mol Biol Evol Doi. doi:10.1093 /molbev/msv265

Kalinin AE, Kajava AV, Steinert PM. 2002. Epithelial barrier function: assembly and structural features of the cornified cell envelope. BioEssays 24: 789–800

Kemp DJ, Dyer PY, Rogers GE (1974) Keratin synthesis during development of the embryonic chick feather. J Cell Biol 62:14–131

Knapp LW, Linser PJ, Carver WE, Sawyer RH (1991) Biochemical identification and immunological localization of two non-keratin polypeptides associated with the terminal differentiation of avian scale epidermis. Cell Tiss Res 265:535–545

Kowata K, Nakaoka M, Nishio K, Fukao A, Satoh A, Ogoshi M, Takahashi S, Tsudzuki M, Takeuchi S (2014) Identification of a feather β-keratin gene exclusively expressed in pennaceous barbule cells of contour feathers in chicken. Gene 542:23–28

Kuraitis KV, Bowers RR (1978) An ultrastructural study of periderm granules in the regenerating feather of the jungle fowl. Cell Tissue Res 192:319–326

Li YI, Kong L, Ponting CP, Haerty W (2013) Rapid evolution of beta-keratin genes contribute to phenotypic differences that distinguish turtles and birds from other reptiles. Genome Biol Evol 5:923–933

Lin CM, Jiang TX, Widelitz RB, Chuong CM (2006) Molecular signaling in feather morphogenesis. Curr Opin Cell Biol 18:730–741

Lin SJ, Widelitz RB, Yue Z, Li A, Wu X, Jiang TX, Wu P, Chuong CM (2013) Feather regeneration as a model for organogenesis. Developm Growth Diff 55:139–148

Lucas AM, Stettenheim PR (1972) Growth of follicles and feathers. Color of feathers and integument. In: Avian anatomy. Integument. Agriculture handbook 362, chapter 7th. US Department of Agriculture, Washington DC, pp 341–419

Maddin HC, Reisz RR (2007) The morphology of terminal phalanges in permo-carboniferous synapsids: an evolutionary perspective. Can J Earth Sci 44:267–274

Maderson PFA (1972a) When? why? and how?: some speculations on the evolution of the vertebrate integument. Amer Zool 12:159–171

Maderson PFA (1972b) On how an archosaurian scale might have given rise to an avian feather. Amer Natur 176:424–428

Maderson PFA, Alibardi L (2000) The development of the sauropsid integument: a contribution to the problem of the origin and evolution of feathers. Amer Zool 40:513–529

Maderson PFA, Hillenius WJ, Hiller U, Dove CC (2009) Toward a comprehensive model of feather regeneration. J Morphol 270:1166–1208

Martin LD, Czerkas SA (2000) The fossil record of feather evolution in the mesozoic. Amer Zool 40:687–694

Matoltsy AG (1987) Cell and Molecular biology of keratins. Concluding remarks and future directions. In Topics in Developmental Biology. 22, (volume editor R.H. SAWYER). Acc. Press Inc. Orlando, FL, USA, pp 255-264

Matulionis DH (1970) Morphology of the developing down feathers of chick embryos. A descriptive study at the Ultrastructural level of differentiation and keratinization. Zeitsch Anat Entwik Gesch 132: 107–157

McKellar RC, Chatterson BDE, Wolfe AP, Curie PJ (2011) A diverse assemblage of late cretaceous dinosaur and bird feathers from Canadian amber. Science 333:1619–1622

Meyer W, Baumgartner G (1998) Embryonal feather growth in the chicken. J. Anat. 193, 611–616

Mischke D, Korge BP, Marenholz I, Volz A, Ziegler A (1996) Genes encoding structural proteins of epidermal cornification and S100 calcium-binding proteins form a gene complex ("epidermal differentiation complex") on human chromosome 1q21. J Invest Dermatol 106:989–992

Mlitz V, Strasser B, Jaeger K, Hermann M, Ghannadan M, Buchberger M, Alibardi L, Tschachler E, Eckhart L (2014) Trichohyalin-like proteins have evolutionarily conserved roles in the morphogenesis of skin appendages. J Invest Dermatol 134:2682–2692

Ng CS, Wu P, Foley J, Foley A, MsDonald ML, Juan WT, Huang CT, Lai YT, Chen CF, Leal SM, Zhang H, Widelitz RB, Patel PI, Li WH,

Chuong CM (2012) The chickem frizzle feather is due to an alpha-keratin (KRT75) mutation that causes a defective rachis. PLoS Genet 8(7):e1002748

Ng CS, Chen CK, Fan WL, Wu P, Wu SM, Chen JJ, Lai YT, Mao CT, Lu MYJ, Chen DR, Lin ZS, Yan KJ, Sha YA, Tu TC, Chen CF, Chuong CM, Li WH (2015) Transcriptome analyses of regenerating adult feathers in chicken. BMC Genomics 16(756):1–16

O'Connors JK, Chiappe LM, Chuong CM, Bottjer DJ, You H (2012) Homology and potential cellular and molecular mechanisms for the development of unique morphologies in early birds. Geosci 2:157–177

Pabisch S, Puchegger S, Kirchner HOK, Weiss IM, Peterlik H (2010) keratin homogeneity in the tail feathers in Pavo cristatus and Pavo cristatus mut. Alba. J Struct Biol 172:270–275

Powell BC, Rogers GE (1979) Isolation of messenger RNA coding for the fast protein of embryonic chick feather. Nucl Acid Res 7:2165–2176

Powell B, Rogers G (1994) Differentiation in hard keratin tissues: hair and related structure. In: Leigh I, Lane B, Watt F (eds) The keratinocyte handbook. Cambridge University Press, Cambridge, pp 401–436

Prin F, Dhouailly D (2004) How and when the regional competence of chick epidermis is established: feathers vs scutate and reticulate scales, a problem en route to a solution. Int J Dev Biol 48:137–148

Prum OR (1999) Development and evolutionary origin of feathers. J Exp Zool 285B:291–306

Prum RO, Brush AH (2002) The evolutionary origin and diversification of feathers. Quart Rev Biol 77:261–295

Prum OR, Williamson S (2001) Theory of the growth and evolution of feather shape. J Exp Zool 291:30–57

Rice RH, Winters BR, Durbin-Johnson PD, Rocke DM (2013) Chicken corneocyte cross-linked proteome. J Prot Res 12:771–776

Rogers MA, Langbein L, Praetzel-Wunder S., Winter H, Schweizer J. 2006. Human keratinassociated proteins (KAPs). Int Rev Cytol 251: 209-262

Romer AS (1941) The skin of the rachitomous amphibian Eryops. Amer J Sci 239:822–824

Sawyer RH, Knapp LW (2003) Avian skin development and the evolutionary origin of feathers. J Exp Zool 298B:57–72

Sawyer RH, Glenn TC, French JO, Mays B, Shames RB, Barnes GL, Rhodes W, Ishikawa Y (2000) The expression of beta (β) keratins in the epidermal appendages of reptiles and birds. Amer Zool 40: 530–539

Sawyer RH, Salvatore BA, Potylicki TT, French JO, Knapp LW (2003) Origin of feathers: feather beta-keratins are expressed in discrete epidermal cell populations of embryonic scutate scales. J Exp Zool 295B:12–24

Sawyer RH, Rogers L, Washington L, Glenn TC, Knapp LW (2005) Evolutionary origin of the feather epidermis. Dev Dyn 232:256–267

Spearman RIC, Hardy JA (1985) Integument. In: King AS, McLelland J (eds) Form and function of birds, vol 3. Academic, London, pp 1–56

Steinert PM, Freedberg IM (1991) Molecular and cellular biology of keratins. In: Goldsmith LA (ed) Physiology, biochemistry, and molecular biology of the skin. Oxford University Press, New York, pp 113–147

Strasser B, Mlitz V, Hermann M, Rice RH, Alibardi L, Tschachler E, Eckhart L (2014) Evolutionary origin and diversification of epidermal barrier proteins in amniotes. Molec Biol Evol 31:3194–3205

Strasser B, Mlitz V, Hermann M, Tschachler E, Eckhart L (2015) Convergent evolution of cysteine-rich proteins in feathers and hair. BMC Evol Biol 15(82):1–11

Sugiyama S, Takahashi M, Kamimura M (1976) The ultrastructure of the hair follicle in early and late catagen, with special references to the alteration of the junctional structure between the dermal papilla and epithelial component. J Ultrastr Res 54:359–373

Sumida SS, Brochu CA (2000) Phylogenetic context for the origin of feathers. Amer Zool 40:486–503

Toni M, Dalla Valle L, Alibardi L (2007) Hard (beta)keratins in the epidermis of reptiles: composition, sequence and molecular organization. J Prot Res 6:3377–3392

Vanhoutteghem A, Djian P, Green H (2008) Ancient origin of the gene encoding involucrin, a precursor of the cross-linked envelope of epidermis and related epithelia. PNAS 105:15481–15486

Widelitz RB, Jiang TX, Yu M, Shen T, Shen JY, Wu P, Yu Z, Chuong CM (2003) Molecular biology of feather morphogenesis: a testable model for evo-devo research. J Exp Zool 298B:109–122

Wu P, Ng CS, Yan J, Lai YC, Chen CK, Lai YT, Wu SM, Chen JJ, Luo W, Widelitz RB, Li WH, Chuomg CM (2015) Topographical mapping of α-and β-keratins on developing chicken skin integument: functional interaction and evolutionary perspectives. PNAS.doi: 10.1073 /pnas.1520566112.

Wyld JA, Brush AH (1979) The molecular heterogeneity and diversity of reptilian Keratins. J Molec Evol 12: 331-347

Wyld JA, Brush AH (1983) Keratin diversity in the reptilian epidermis. J Exp Zool 225: 387-396

Yu M, Wu P, Widelitz RB, Chuong CM (2002) The morphogenesis of feathers. Nature 420:308–312

Yu M, Yue Z, Wu P, Wu DY, Mayer JA, Medina M, Widelitz RB, Jiang TX, Chuong CM (2004) The developmental biology of feather follicle. Intern J Dev Biol 48:181–191

Yue Z, Jiang TX, Widelitz RB, Chuong CM (2005) Mapping stem cell activities in the feather follicle. Nature 438:1026–1029

Yue Z, Jiang TX, Widelitz RB, Chuong CM (2006) Wnt3a gradient converts radial to bilateral feather symmetry via topological arrangement of epithelia. PNAS 103:951–955